ตรวจการกลายพันธุ์ของเอ็กซอน 11 ในยีน *c-kit* ด้วยเทคนิคพีซีอาร์จากเซลล์เนื้องอกมาสต์เซลล์ที่ผิวหนังของสุนัขที่เก็บโดยวิธีการเจาะดูด

นายเดชธชัย เกตุพันธุ์

วิทยานิพนธ์นี้เป็นส่วนหนึ่งของการศึกษาตามหลักสูตรปริญญาวิทยาศาสตรมหาบัณฑิต
สาขาวิชาพยาธิชีววิทยาทางสัตวแพทย์ ภาควิชาพยาธิวิทยา
คณะสัตวแพทยศาสตร์ จุฬาลงกรณ์มหาวิทยาลัย
ปีการศึกษา 2554

DETECTION OF EXON-11 MUTATION IN *c-kit* USING PCR TECHNIQUE FROM CANINE CUTANEOUS MAST CELL TUMORS OBTAINED BY FINE-NEEDLE ASPIRATION METHOD

Mr. Dettachai Ketpun

A Thesis Submitted in Partial Fulfillment of the Requirements

for the Degree of Master of Science Program in Veterinary Pathobiology

Department of Veterinary Pathology

Faculty of Veterinary Science

Chulalongkorn University

Academic Year 2011

Thesis Title	DETECTION OF EXON-11 MUTATION IN *c-kit* USING PCR TECHNIQUE FROM CANINE CUTANEOUS MAST CELL TUMORS OBTAINED BY FINE-NEEDLE ASPIRATION METHOD
By	Mr. Dettachai Ketpun
Field of Study	Veterinary Pathobiology
Thesis Advisor	Associate Professor Achariya Sailasuta D.V.M., Ph.D.
Thesis Co-advisor	Prapruddee Piyawiriyakul D.V.M., M.Sc., Ph.D.

Accepted by the Faculty of Veterinary Science, Chulalongkorn University in Partial Fulfillment of the Requirements for the Master's Degree

…….…….. Dean of the Faculty of Veterinary Science
(Professor Mongkol Techakumphu, D.V.M., Doctorate de 3e cycle)

THESIS COMMITTEE

…….. Chairman
(Associate Professor Anudep Rungsipipat D.V.M., Ph.D.)

……. Thesis Advisor
(Associate Professor Achariya Sailasuta D.V.M., Ph.D.)

…….. Thesis Co-advisor
(Prapruddee Piyawiriyakul D.V.M., M.Sc., Ph.D.)

…….. External Examiner
(Assistant Professor Chaiyan Kesorndorkbua D.V.M., Ph.D.)

เดชธชัย เกตุพันธุ์: ตรวจสอบการกลายพันธุ์ของเอ็กซอน 11 ในยีน *c-kit* ด้วยเทคนิคพีซีอาร์จากเซลล์เนื้องอกมาสต์เซลล์ที่ผิวหนังของสุนัขที่เก็บโดยวิธีการเจาะดูด (DETECTION OF EXON-11 MUTATION IN *c-kit* USING PCR TECHNIQUE FROM CANINE CUTANEOUS MAST CELL TUMORS OBTAINED BY FINE-NEEDLE ASPIRATION METHOD) **อ. ที่ปรึกษาวิทยานิพนธ์หลัก: รศ. สพ.ญ. ดร. อัจฉริยา ไศละสูต, อ. ที่ปรึกษาวิทยานิพนธ์ร่วม: อ. น.สพ. ดร. ประพฤติดี ปิยะวิริยะกุล, 73 หน้า.**

งานวิจัยนี้มีวัตถุประสงค์เพื่อตรวจสอบการกลายพันธุ์ของเอ็กซอน 11 ที่อยู่ในโปรโตออนโคยีน *c-kit* ด้วยวิธีพีซีอาร์ จากเซลล์เนื้องอกมาสต์เซลล์ของสุนัขที่เก็บโดยวิธีการเจาะดูดเซลล์ในสุนัขที่เป็นเนื้องอกมาสต์เซลล์ที่ผิวหนังจำนวน 30 ตัวอย่าง สุนัขที่นำมาศึกษาทั้งหมดจะถูกเก็บตัวอย่างชิ้นเนื้อเพื่อวินิจฉัยและแบ่งเกรดของเนื้องอกมาสต์เซลล์ทางจุลพยาธิวิทยาโดยใช้ระบบการแบ่งเกรดเนื้องอกมาสต์เซลล์ทางจุลพยาธิวิทยาของ Patniak เป็นมาตรฐาน และตัวอย่างชิ้นเนื้อของสุนัขแต่ละตัวอย่างที่เก็บมาได้ยังนำมาศึกษารูปแบบการติดสีของโปรตีน KIT (CD117) ด้วยวิธีทางอิมมูโนฮีสโตเคมีด้วยเพื่อใช้เป็นเกณฑ์มาตรฐานสำหรับวิเคราะห์ผลการย้อมสีโปรตีน KIT ด้วยวิธีอิมมูโนไซโตเคมี และเซลล์เนื้องอกมาสต์เซลล์ที่เก็บได้ด้วยวิธีการเจาะดูดนั้นจะนำมาทำให้อยู่ในรูปสารแขวนลอยของเซลล์ เพื่อใช้สำหรับตรวจสอบการกลายพันธุ์ของเอ็กซอน 11 ที่อยู่ในโปรโตออนโคยีน c-kit ต่อไป จากการใช้เทคนิคโฟว์ไซโตเมตรี้ในการวิเคราะห์หาปริมาณของเซลล์เนื้องอกมาสต์เซลล์ของสุนัขในสารแขวนลอยของเซลล์จำนวน 15 ตัวอย่างก่อนทำพีซีอาร์พบว่า ในสารแขวนลอยของเซลล์เนื้องอก 1 ไมโครลิตรนั้นจะมีจำนวนของเซลล์เนื้องอกมาสต์เซลล์ที่เก็บโดยการเจาะดูดในสารแขวนตะกอนของเซลล์เฉลี่ยอยู่ที่ 6,345 เซลล์ (6.345×10^6 เซลล์ต่อมิลลิลิตร) เซลล์เนื้องอกที่ได้จากการเจาะดูดนี้ส่วนหนึ่งจะนำมาย้อมสีโปรตีน KIT ด้วยวิธีทางอิมมูโนไซโตเคมีเพื่อศึกษารูปแบบการติดสีของโปรตีน KIT และอีกส่วนหนึ่งจะนำมาสกัดแยกสารพันธุกรรมเพื่อใช้ในการทำพีซีอาร์ต่อไป ผลของการศึกษาชี้ให้เห็นว่า รูปแบบการติดสีของโปรตีน KIT ที่ย้อมด้วยวิธีทางอิมมูโนไซโตเคมีนั้นจะมีรูปแบบที่เหมือนกันกับที่พบในเนื้อเยื่อตัวอย่างของเนื้องอกมาสต์เซลล์ที่ย้อมสีโปรตีน KIT ด้วยวิธีทางอิมมูโนฮีสโตเคมี โดยรูปแบบการติดสีมี 3 แบบคือ ติดสีรอบเยื่อหุ้มเซลล์ ติดสีรวมกลุ่มกันในไซโตปลาสมใกล้นิวเคลียสของเซลล์เนื้องอก หรือติดสีกระจายอยู่ทั่วไซโตปลาสมของเซลล์เนื้องอก ผลการศึกษายังแสดงให้เห็นว่าในตัวอย่างแต่ละราย จะมีรูปแบบการติดสีของโปรตีน KIT ที่เหมือนกันทั้งในเซลล์เนื้องอกที่ได้จากการเจาะดูด และในเนื้อเยื่อ โดยมีเพียงตัวอย่างเดียวที่ให้ผลการติดสีที่แตกต่างกัน ชี้ให้เห็นว่าเซลล์เนื้องอกที่ได้จากการเจาะดูดน่าจะเป็นตัวแทนที่ดีของเซลล์เนื้องอกที่อยู่ในเนื้อเยื่อ ในส่วนของการทำพีซีอาร์เพื่อตรวจสอบการกลายพันธุ์ของเอ็กซอน 11 ที่อยู่ในโปรโตออนโคยีน *c-kit* นั้นพบว่า ตัวอย่างของเซลล์เนื้องอกที่ได้จากการเจาะดูดจำนวน 1 ตัวอย่างซึ่งเป็นเนื้องอกมาสต์เซลล์เกรด 2 นั้นให้ผลเชิงบวก โดยตรวจพบการกลายพันธุ์ของเอ็กซอน 11 ที่อยู่ในโปรโตออนโคยีน *c-kit* ในตัวอย่างดังกล่าว ในขณะที่ตัวอย่างที่เหลือตรวจไม่พบการกลายพันธุ์ รวมทั้งผลการศึกษาเปรียบเทียบในการทำพีซีอาร์จากตัวอย่างของเซลล์เนื้องอกมาสต์เซลล์ที่เก็บได้โดยตรงจากก้อนเนื้องอกด้วยการเจาะดูดเซลล์ กับเซลล์เนื้องอกมาสต์เซลล์ที่ย้อมติดสีของโปรตีน KIT และถูกคัดกรองออกมาจากเครื่องโฟว์ไซโตมีเตอร์จากสุนัขตัวอย่างจำนวน 1 ราย ผลการศึกษาแสดงให้เห็นว่าผลพีซีอาร์ของเซลล์เนื้องอกจากทั้ง 2 แหล่งไม่มีความแตกต่างกัน ดังนั้นชี้ให้เห็นว่าเซลล์เนื้องอกมาสต์เซลล์ที่เก็บได้โดยตรงจากก้อนเนื้องอกนั้นสามารถใช้เป็นตัวแทนของเซลล์เนื้องอกมาสต์เซลล์ในก้อนเนื้องอก และสามารถนำมาใช้ในการตรวจสอบการกลายพันธุ์ของเอ็กซอน 11 ในโปรโตออนโคยีน *c-kit* ได้ ดังนั้นจึงสรุปได้ว่าเซลล์เนื้องอกมาสต์เซลล์ของสุนัขที่เก็บได้โดยวิธีการเจาะดูดนั้นสามารถนำมาใช้ในการตรวจสอบการกลายพันธุ์ของเอ็กซอน 11 ในโปรโตออนโคยีน *c-kit* เบื้องต้นในทางคลินิกได้ แต่ความแม่นยำของวิธีการรวมทั้งการนำไปประยุกต์ใช้ในการวินิจฉัย และวางแผนรักษาเนื้องอกมาสต์เซลล์ในระดับคลินิกนั้นยังคงต้องมีการศึกษาเพิ่มเติมและควรจะมีการวางแผนขั้นตอนในการศึกษาให้รัดกุมต่อไป และควรจะศึกษาในตัวอย่างที่มีจำนวนมากขึ้นเพื่อให้ได้ผลที่แน่นอน ก่อนที่จะนำวิธีดังกล่าวไปประยุกต์ใช้ต่อไป

ภาควิชา พยาธิวิทยา ลายมือชื่อนิสิต.....

สาขาวิชา พยาธิชีววิทยาทางสัตวแพทย์ ลายมือชื่อ อ.ที่ปรึกษาวิทยานิพนธ์หลัก.....

ปีการศึกษา 2554 ลายมือชื่อ อ.ที่ปรึกษาวิทยานิพนธ์ร่วม.....

5275558931: MAJOR VETERINARY PATHOBIOLOGY
KEYWORDS: CANINE CUTANEOUS MAST CELL TUMORS / FINE NEEDLE ASPIRATION / FLOW CYTOMETRY / PCR / EXON 11 IN *c-kit*

DETTACHAI KETPUN: DETECTION OF EXON-11 MUTATION IN *c-kit* USING PCR TECHNIQUE FROM CANINE CUTANEOUS MAST CELL TUMORS OBTAINED BY FINE-NEEDLE ASPIRATION METHOD. ADVISOR: ASSOC. PROF. ACHARIYA SAILASUTA D.V.M., Ph.D., CO-ADVISOR: PRAPRUDDEE PIYAWIRIYAKUL D.V.M., M.Sc. Ph.D., 73 pp.

This research has been objectively set up to study the usage of MCT cells collected by fine-needle aspiration (FNA) method for investigating mutant exon-11 in proto-oncogene *c-kit* from 30 MCT dogs. All studied MCT dogs were performed tissue biospsy for MCT histopathologic diagnosis and grading using Patniak histopathologic grading system. All biopsied tissues were also studied the staining patterns of KIT (CD117) by CD117-immunohistochemitry. The result was used as the standard criteria for CD117-immunocytochemistry interpretation. For fine-needle aspirated MCT cells (FNA-MCT cells) in cell suspensions, they were used further for study in detection of mutant exon-11 in *c-kit*. From flow cytometric quantitative analysis in fifteen FNA-MCT cell suspensions, the result suggested that there were approximately 6,345 FNA-MCT cells in 1 μl of cell suspensions (6.345×10^6 cells/ ml). FNA-MCT cells were used for 2 purposes; the first for CD117-immunocytochemistry study and the last for DNA extraction used in PCR study. The result from CD117-immunocytochemistry indicated that the staining patterns of KIT mimic to the staining patterns observed in CD117-immunohistochemistry consisting of perimembrane, paranuclear and cytoplasmic diffuse. Moreover, the consequence also indicated that each specimen also possessed the same staining pattern both in CD117-immunocytochemistry and CD117-immunohistochemistry except in one specimen having the different result. This suggested that FNA-MCT cells should be representative of neoplastic cells in biopsied tissues. For PCR analysis, one FNA-MCT specimen classified as MCT-grade II by histopathology gave the positive outcome by detecting the mutant exon-11 in *c-kit* with PCR. In the comparative study of PCR analysis for mutant exon-11 in c-kit from FNA-MCT cells collected directly from the tumor mass with FNA-MCT cells sorted through flow cytometric cell sorter in one case, the results were not different from each other indicating that FNA-MCT cells directly obtained from the tumor mass should be the representative of MCT-cell populations in the biopsied tissue. In addition, they could be preliminarily applied for clinical detection of mutant exon-11 in *c-kit* by PCR. However, a mass study for further investigating the consistency of this method should be executed before this method will be clinically applied for MCT diagnosis and therapeutic planning.

Department : Veterinary Pathology ..... Student's Signature .....

Field of Study : Veterinary Pathobiology ..... Advisor's Signature .....

Academic Year : 2011 ..... Co-advisor's Signature .....

ACKNOWLEDGEMENTS

Firstly, I would like to thank Department of Veterinary Pathology, Faculty of Veterinary Science, Chulalongkorn University for acceptance me to take the great opportunity for developing myself in the field of Veterinary Pathobiology. Secondly, I would like to send my gradtitude to my thesis principal advisor, Assoc. Prof. Dr. Achariya Sailasuta, who encourages me for everything both on the stage and at the back stage. I also appreciate my thesis co-advisor, Dr. Papruddee Piyawiriyakul, for all helpful associations when I got tough lives especially on the laboratory processes. Additionally, I would like to thank Prof. Dr. Roongroje Tanawongnuvej, the head of department, Assoc. Prof. Dr. Anudep Rungsipipat and Assoc. Prof. Dr. Wijit Bunloonara with their special supervisions to me. Endlessly, I would like to acknowledge my three lecturers from Faculty of Veterinary Medicine, Kasetsart University; Assoc. Prof. Dr. Saree Dornkaewbua who was the first person triggering me to be interested in Veterinary Pathology, Assoc. Prof. Dr. Taweesak Songserm who has been empowering me to study in Veterinary Pathology, and Assist. Prof. Dr. Chaiyan Kesorndorkbua who is my idol for study in Veterinary Pathology, as well as I would like to thank all lectures and staffs from Department of Veterinary Pathology, Faculty of Veterinary Science, Chulalongkorn University for giving me the great knowledge in Veterinary Pathology, including with all lecturers from Faculty of Veterinary Science, Chulalongkorn University and Faculty of Veterinary Medicine, Kasetsart University, who have given me the best basis in all veterinary fields.

Specially, I would like to thank Prof. Dr. Vilma Yuzbasiyan-Gurkan and Dr. Tuddow Thaiwong from College of Veterinary Medicine, Michigan State University for their kindness on PCR primer sequences, the positive control and normal control provisions, including Assoc. Prof. Dr. Matti Kiupel from the same institution for his useful comments. I also acknowledge Dr. Kowit Pattanapanyasat and Dr. Nuttawat Onlamoon from Faculty of Medicine, Sririraj Hospital, Mahidol University for their great collaborations in Flow-Cytometry. So many times, I would like to thank Dr. Pattarakij Theewasutrakul, Dr. Kasemsri Satjawiriyakul and Dr. Pat Kormanee for specimen monitoring and collection. The next appreciation is issued to Dr.Nognuj Auiwawongsak and Mr. Anusorn Kaneungthong for your helpful associations in my last laboratory period. Moreover, I would like to acknowledge the Rajchadapiseksompoj research fund from Chulalongkorn University and STAR research fund from Faculty of Veterinary Science, Chulalongkorn University for your financial supports.

Ultimately and endlessly, I would like to thank my father and my mother for your backup bringing me about the victory in this study as well as with the special thank to my wife, son and daughter for your encouraging and patience along my study.

CONTENTS

LIST OF TABLES

LIST OF FIGURES

LIST OF ABBREVIATIONS

%	Percent
AD	Atopic Dermatitis
AgNORs	Argyrophillic Nuclear Organizing Region proteins
BSA	Bovine Serum Albumin
c3	Complement 3
c5	Complement 5
cc	Cubic Centimeter
CD13	Cluster of Different 13
CD34	Cluster of Different 34
CD45	Cluster of Different 45
CD117	Cluster of Different 117
COX	Cyclo-Oxygenase
DAB	Diaminoenzidine Tetrahydrochloride
dATP	Adenosine Triphosphate
dCTP	Cytosine Triphosphate
dGTP	Guanine Triphosphate
DNA	Deoxyribonucleic Acid

dNTP	Deoxy-nucleotide Triphosphate
dTTP	Thymine Triphosphate
ECF-A	Eosinophillic Chemoattraction Factor of Anaphylaxis
FCM	Flow Cytometry
FcεRI	Immunoglobulin E-Fc receptor type 1
FcγRI	Immunoglobulin G-Fc receptor type 1
FGF	Fibroblast Growth Factor
FNA	Fine-Needle Aspiration or Fine-Needle Aspirated
FNA-MCT	Fine-Needle Aspirated-Mast Cell Tumors
GM-CSF	Granulocyte Monocyte-Colony Stimulating Factor
H&E	Hematoxylin and Eosin
H_2O_2	Hydrogen Peroxide
HCl	Hydrochoric Acid
HPF	High Power Field
KCl	Potassium Chloride
ICAM	Intercellular Adhesion Molecule
ICC	Immunocytochemistry

IFN	Interferon
IgE	Immunoglobulin Epsilon
IgG	Immunoglobulin Gamma
IHC	Immunohistochemistry
ITD	Internal Tandem Duplication
kDa	Kilo-Dalton
LFA	Leukocyte Function-associated Antigen
LOX	Lipoxygenase
LT	Leukotriene
LTC_4	Leukotriene C_4
LTD_4	Leukotriene D_4
LTE_4	Leukotriene E_4
M	Molar
MAdCAM-1	Mucosal Address in Cell Adhesion Molecule-1
MCP-1	Monocyte Chemoattraction Protein-1
MCT	Canine Cutaneous Mast Cell Tumors
MgCl2	Magnesium Chloride
MGF	Mast Cell Growth Factor

MIP-1α	Macrophage inflammatory Protein-1 Alpha
ml	Milliliters
mM	Millimolar
mRNA	Messenger Ribonucleic Acid
NGF	Nerve Growth Factor
$(NH_4)_2SO_4$	Ammonium sulfate
NO	Nitric Oxide
^oC	Celcius degree
PAF	Platelet Activating Factor
PAS	Periodic Acid fast Stain
PCNA	Proliferating Cell Nuclear Antigen
PCR	Polymerase Chain Reaction
PDGF	Platelet-Derived Growth Factor
PGD_2	Prostaglandin D_2
RTK	Receptor Tyrosine Kinase
RT-PCR	Reverse Transcriptase-Polymerase Chain Reaction
SCF	Stem Cell Factor
TF	Transcription Factor

TGF-β	Transforming Growth Factor-Beta
T_H2	Helper T Cells type 2
TKI	Tyrosine Kinase Inhibitor
TNF-α	Tumor Necrosis Factor-Alpha
TVT	Transmissible Venereal Tumors
VCAM-1	Vascular Cell Adhesion Molecule-1
VEGF	Vascular Endothelial Growth Factor
μg	Micrograms
μl	Microliters
μmol	Micromolar
1X	one-fold
10X	ten-fold
400 X	four hundred-fold

CHAPTER I

INTRODUCTION

Canine cutaneous mast cell tumor (MCT) is the second most canine cutaneous tumors. The incidence of the tumor has been reportedly accounted for 7-21%. So far, the exact tumorigenesis of MCT is poorly understood and it is proposed to be multifactorial. Moreover, biological behaviors of MCT tumor cells are very varied even in the same histopathological grade. Basically, MCT patients often suffer not only from a tumor invasion to deeper tissues but also from paraneoplastic syndromes due to an excessive release of various biological chemomediators stored in intracytoplasmic granules. Although, paraneoplastic syndromes can be manageable; however in some cases, paraneoplastic syndromes cause a fatal effect to MCT patients; for examples, a gastrointestinal perforation leading to peritonitis or an acute heart failure caused by generalized vasodilatation owing to an excessive histamine release (London and Seguin, 2003; Thamm and Vail, 2007). Therefore, MCT patients are generally required a swift diagnostic and prognostic protocol to prevent the death.

Eventhough, The gold standard protocol for diagnosis and prognosis for MCT is recently based on Patnaik histopathologic grading system (Thamm and Vail, 2007; Welle et al., 2008). However, the method is invasive and time-consuming and the method also traumatizes in which very harmful to moribund MCT dogs. Although recently, there have been many endeavors to establish alternative diagnostic and prognostic protocols; such as AgNORs-, PCNA-, and Ki-67-immunohistochemistry to diagnose and prognosticate MCT (Zemke et al., 2002; Kiupel et al., 2004; Dobson and Scase 2007; Newman et al., 2007). However, these protocols still lack of the specific cut-off values on MCT grading and prognosticating (Kiupel et al., 2004) as well as they are required well-trained pathologists to perform, because interpretations are varied among veterinary pathologists. Therefore, the most favorite diagnostic and prognostic protocol is still being Patnaik histopathologic grading system. Fine-needle aspiration (FNA) to date is one alternative diagnostic tool for MCT. Although, Fine-needle aspiration can provide a rapid screening diagnosis for MCT clinically; however, FNA still has disadvantages; for examples, it obtains a low number of MCT cells with a little information on grading and prognosticating for MCT. On the other hand, FNA still has a

benefit for MCT diagnosis, because it is the low cost, painless, convenient and less harmful protocol than other diagnostic and prognostic methods motioned above. So, it is currently suitable for use in the screening diagnosis for MCT. CD117-immunohistochemistry (CD117-IHC) has been reportedly shown the efficacy on MCT diagnosis especially MCT in a transitional stage. However, the protocol is also required biopsy which is invasive and painful as well as the method is needed suitable anesthetic protocols leading to MCT patients, particularly vulnerable MCT patients might be at risks on the protocol. In order to enhance the ability of FNA for diagnosis MCT, probably CD117-antibodies used in CD117-immunohistochemistry might be applied for CD117-immunocytochemistry for being used in diagnosing MCT from FNA-MCT cells. One preliminary study has exhibited that the staining patterns of KIT in CD117-immunocytochemistry performed on FNA-MCT cells were identical to those seen in CD117-immunohistochemistry (Theerawatanasirikul et al., 2009).

According to the exact MCT pathogenesis has been less-well established and is proposed to be multi-factorial. However, the results in previous studies suggesting that the proto-oncogene *c-kit* has contributed in MCT tumorigenesis as found in case of human mastocytosis (Letard et al., 2008). This proto-oncogene encodes for KIT proteins which are the member of class III-receptor protein tyrosine kinase (class III-RTK) presenting on plasma membranes of mast cells (Roskoski, 2005). Recently, there have been many evidences showing the activating mutation of exon-11 in *c-kit* causes constitutively autophosphorylation of KIT in MCT, leading to an uncontrollable proliferation for MCT tumor cells (London et al., 1999; Ma et al., 1999; Zemke et al., 2001; Zemke et al., 2002; Jones et al., 2004; Kiupel et al., 2004; Turin et al., 2006; Webster et al., 2006; Letard et al., 2008). Therefore, mutated exon-11 in *c-kit* might be a one critical factor in MCT tumorigenesis. Furthermore, the mutation of exon-11 in *c-kit* also affects the efficacy of a novel receptor tyrosine kinase inhibitor such as Toceranib (Palladia™, SU11654) which this agent prevents a phosphorylation on the tyrosine residues at the ATP-binding sites of KIT leading to an inhibiting of downward cascades in KIT-intracellular signaling. In order to study mutation of exon-11 in *c-kit*, the standard PCR has been employed in almost studies. However, the MCT specimens are still come from biopsy of which invasive, pain, harmful and time-consuming. Owing to therapeutic protocols are dependently based on MCT histopathologic grade and prognosis. Therefore, accurate grading and

prognosticating protocols are still essential for MCT therapy. It means the safety of MCT patients. Based upon previous information, the questions in this study were;

1. Could we use FNA-MCT cells to study exon-11 mutation in *c-kit* with standard PCR?

2. Could we use Flow cytometry to perform Flow cytometric quantitative analysis for FNA-MCT cells in a cell suspension before proceeding PCR?

Accordingly, the hypotheses of this study were set up on the basis of FNA can effectively used for obtaining MCT cells from a MCT mass and these FNA-MCT cells could be applied for study exon-11 mutation in *c-kit* using PCR. In addition, Flow cytometry can facilitate the study in enumeration FNA-MCT cells in a cell suspension. Hence, the objectives of this study were to demonstrate that the standard PCR-based protocol could be used for study exon-11 mutation in *c-kit* from FNA-MCT cells and to set up a well-established protocol used in Flow cytometric quantitative analysis for FNA-MCT cells in a cell suspension. Moreover, the expected outcome from PCR analysis might be associated to CD117-immunohistochemistry and CD117-immunocytochemistry.

CHAPTER II

LITERATURE REVIEW

2.1 Histology and cytology of normal mast cells

Mast cells are phylogenitically old cells. They had been firstly observed by Von Recklinghausen in 1863 and were named by Paul Ehrlish as Mastzellen (Well-Fed cells) in 1878. They were described as the cell containing phagocytosed material or nutrients inside their cytoplasmic granules (Hill and Martin, 1998; Moldering, 2010). Mast cells are tissue-based inflammatory cells found in all mammals (Prussin and Metcalfe, 2006; Moldering, 2010), which they have been previously identified as the tissue basophils leading to a misconception about mast cell origin even in modern textbooks to date (Hill and Martin, 1998).

Basically, mast cells are scanty in the parenchymatous tissues (Prussin and Metcalfe, 2003) but highly seen at tissue interfaces to external milieus (Hill and Martin, 1998; Prussin and Metcalfe, 2006). In general, they reside in the loose connective tissues of skin, respiratory tract, heart, brain, liver, testes, nerve ending and gastrointestinal tract (Hill and Martin, 1998; Eurell and Van Stickle, 2006; Mora et al., 2006). In canine, mast cells are densely distributed in the stomach and duodenum (Mora et al., 2006). In lung, they are in the bronchial connective tissues adjacent to the epithelium and in alveolar spaces (Prussin and Metcalfe, 2006). Of the canine skins, they usually reside near the hair follicles especially at the dermo-epidermal junctions closed to the hair follicle bases (Mora et al., 2006), sebaceous glands and sweat glands of skins (Prussin and Metcalfe, 2006). In addition, they are abundantly found around the venules and the deeper dermis, as well as in the adipose tissue of subcutis. The distribution of mast cells in uterus and lymph nodes in canine species are scarce (Mora et al., 2006).

Mast cells in canine and feline species are recently classified into three distinguished subpopulations; mucosal mast cells (MMC or MC_T) found mainly in the alimentary and respiratory tracts, connective tissue mast cells (CTMC or MC_{TC}) in the skins (Maria and Zorn 2003; Eurell and Van Stickle, 2006; Mora et al., 2006) and the third mast cell type (MC_C) which seen mainly

in the subepithelial and periadnexal areas of skins preserved by a special fixation such as Carnoy's fixative, respectively (Eurell and Van Stickle, 2006; Mora et al., 2006). The classification is therefore based upon the immunohistochemistry property of neutral proteases contained in mast cells (Mora et al., 2006; Prussin and Metcalfe, 2006). By this method, the difference between each group is therefore depending on their granular contents and their residential sites. In mucosal mast cells, their granules contain only tryptase but in connective tissue mast cells contain not only tryptase but also chymase, carboxypeptidase-A and cathepsin-D. Meanwhile, the third mast cell type, their granules contain chymase and carboxypeptidase-A (Lee et al., 1985; Mora et al., 2006). However, almost mast cells commonly found in dogs and cats are connective tissue and mucosal mast cells (Lee et al., 1985; Mora et al., 2006).

Morphologically, mast cells are round to oval in shape with approximately 8-30 μm in diameter. The size is variably observed depending on their tissue sources (Maria and Zorn, 2003; Moldering, 2010). For instance, the dimension of mast cells is 16.2 ± 0.11 μm, 15.2 ± 0.3 μm, 14.3 ± 0.5 μm, 14.1 ± 0.5μm, 13.1 ± 0.6 μm and 12.0 ± 0.6 μm in the external anal sphincter, lamina propria, anal glands, internal anal sphincter, sebaceous glands of anus and sudoriferous glands, respectively (Stefanov et al., 2007). At the meantime, the diameter of skin mast cells is ranged from 12-14 μm (Mora et al., 2006).

Electronmicroscopically, mast cells are round to elongate cells which compressed to conform to the surrounding tissues. The nuclei are oval but in some stage are irregularly indent. The nuclei are centrally or eccentrically located in cells. Their cytoplasm usually contains approximately 0.47 μm cytoplasmic granules (Mora et al., 2006). Mast cell granules could be morphologically separated as; crystalline, lamellar, and fine granules under an electron microscopy. The organelles mostly seen are free ribosomes, cisternae of rough endoplasmic reticulum (rER), polysomes and numerous mitochondria (Samuelson, 2007; Moldering, 2010). In addition, mast cells generally possess F-actin filaments underlying their cytoplasmic membranes. This cytoskeletal protein is crucial for mast cell degranulation (Hill and Martin, 1998).

Histologically, mast cells are round to oval in shape. The nuclei are centrally situated and spherical to oval in shape (Maria and Zorn, 2003). The cytoplasm generally contains

membrane-bounded basophilic-refractile granules (Leeson et al., 1985; Samuelson, 2007). However, in some histological preparation, mast cells do not contain these granules owing to the preparatory processes abolishing them from the cells but these granules could be readily found in surrounding tissues which close to those mast cells (Li, 2001). According to previous studies, canine mast cells are morphologically and functionally resemblance to human mast cells suggesting that mast cells are conserved across both species (Mora et al., 2006).

Basically, the cytoplasmic granules of mast cells contain diverse preformed-water soluble chemomediators inside. Almost cytoplasmic granules contain sulfated-glycosaminoglycan such as heparin (proteoglycan heparin) and chondroitin sulfate-E causing matachromasia (Hill and Martin, 1998; Mora et al., 2006; Moldering, 2010). Metachromasia is characterized by heparinic granules are stained in purple-red or pinkish-purplish (metachromatic granules) by basic aniline/thiazine dyes, such as toluidine blue, methylene blue, new methylene blue and azure-A (Leeson et al., 1985; Eurell and Van, 2006; Maria and Zorn, 2003; Stickle, 2006; Meyer et al., 2010; Moldering, 2010). The relative amount of each sulfated proteoglycan might influence in the staining-related properties belonging to CTMC and MMC, as well (Mora et al., 2006). Nevertheless, these cytoplasmic granules also stain with periodic acid fast stain (PAS) (Leeson et al., 1985).

The other preformed chemomediators recently reported in mast cells are carboxypeptidase-A (Prussin and Metcalfe, 2006; Moldering, 2010), neutral serine proteases such as tryptase (110-130 kDa) and chymase (Prussin and Metcalfe, 2006), eosinophilic chemotactic factor of anaphylaxis (ECF-A), β-hexosaminidase (Mora et al., 2006), histamine (Samuelson, 2007) and serotonin in some mammalian species (Leeson et al., 1985). Although, the function of tryptase *in vivo* has not exactly identified, but *in vitro* it functionally cleaves C3 and C3a, recruits inflammatory cells in to an injured site, and activates fibroblasts. Interestingly, 83% of the amino acid sequence of canine chymase is homology to human chymase (Mora et al., 2006). In addition, mast cells could be positively stained by CCR3-, CCR5-, $CXCR_2$- and $CXCR_4$-immunohistochemistry suggesting that they express these chemokine receptors on their cell membranes (Prussin and Metcalfe, 2003). These chemokine receptors are responsible for eotaxin, macrophage inflammatory protein-1α (MIP-1α), IL-8 and stromal cell-derived factor-1 (Austen and Boyce, 2001).

Canine mast cells can also immediately synthesize *de-novo* chemomediators after receiving stimuli, such as antigens and calcium-ionophore A23187. These chemomediators usually named as newly-synthesized chemomediators of mast cells (Mora et al., 2006). There are two kinds of *de-novo* newly-synthesized chemomediators have been identified, so far. The first are lipid-mediated compounds such as leukotriene-B_4 (LTB_4), leukotriene-C_4 (LTC_4), leukotriene-D_4 (LTD_4) and leukotriene-E_4 (LTE_4), also called slow-reacting substances of anaphylaxis or SRS-A, synthesized via lipoxygenase pathway (Maria and Zorn, 2003; Mora et al., 2006; Moldering, 2010) and prostaglandin-D_2 (PGD_2) via cyclooxygenase (COX, PGH synthase) pathway (Mora et al., 2006; Moldering, 2010). The last *de-novo* chemomediator is a group of various cytokines produced from mast cells under various pathophysiological responses such as platelet activating factor (PAF), macrophage inflammatory protein-1α and β (MIP-1α or CCL3; and MIP-1β), monocyte chemoattractant protein-1 (MCP-1) (Moldering, 2010), interferon-α, β and γ (IFN-α, β and γ), tumor necrotic factor-α (TNF-α), leptin, interleukine- (IL-) 1, 3, 4, 5, 6, 8, 9, 10, 12, 13, 14, 16, 18 and 25. These chemomediators are important for physiological and pathophysiological processes responding for tissue homeostasis, injury and inflammation (Moldering, 2010). For example, IL-4 promotes T_H2 differentiation meanwhile IL-5 enhances eosinophil development and its survival. Mast cells also produce IL-1 which has an anti-inflammatory effect. TNF-α is the one of major cytokines produced from mast cells. This cytokine is found as preformed and newly-synthesized cytokines in mast cells (Prussin and Metcalfe, 2006). TNF-α upregulates the initial cytokine cascades responsible for the expression of intercellular adhesion molecule-1 (ICAM-1) by canine endothelial cells and cardiac myocytes. IL-6 is upregulated by TNF-α derived from cardiac mast cells for recruiting leukocytes to infiltrate into myocardium in response for infections (Mora et al., 2006). Various mast cell-derived growth factors are produced in mast cells, as well. For instance, stem cell factor (SCF), granulocyte monocyte-colony stimulating factor (GM-CSF), vascular endothelial growth factor (VEGF), fibroblast growth factor (FGF), nerve growth factor (NGF), platelet derived growth factor (PDGF) and nitric oxide (NO). These mast cell-derived growth factors exert as paracrine, autocrine or even endocrine effects of mast cells (Mora et al., 2006; Prussin and Metcalfe, 2006).

In general, mast cells express a batch of membrane receptors. These receptors play on various physiological and pathologic activities. The major receptors recently identified are

FcεRI and KIT (CD117). These two receptor expressions are depending upon the physiological or pathological stage of mast cells. Besides, mast cells also possess various cytokine and chemokine receptors, such as FcγRI (CD64), FcγRIIb (CD32), C3aR, C5aR (CD88), IL-3R, IL-4R, IL-5R, IL-9R, IL-10R, including the receptors for adenosine, GM-CSF, IFN-γ, CCR3, CCR5, CXC_4, and NGF (Mora et al., 2006; Prussin and Metcalfe, 2006). Mast cell longevity is varied from a week to several months. It is longer than basophils. In some tissue preparations, mast cells also exhibit pseudopodia indicating they have motility but very slow (Lee et al., 1985).

2.2 Heterogeneity of mast cells

The heterogeneity occurs owing to the difference in their morphological, histological, biochemical and functional characteristics in mast cells from different anatomical locations suggesting that mast cells might variably respond to diverse stimuli (Hill and Martin, 1998; Mora et al., 2006). Histological heterogeneity of mast cells indicates that mast cells could be merely classified into two subpopulations, connective tissue mast cells (CTMCs) and mucosal mast cells (MMCs), depending on immunohistochemical properties of their granular contents (Hill and Martin, 1998). MMC usually stains blue with alcian blue meanwhile CTMC stains red with safranin, for example. Therefore, these two dyes are useful to separate MMC from CTMC (Hill and Martin, 1998). MMC in the gastrointestinal tracts predominantly produce more PGD_2 than LTC_4 which contrast to those found in lung, suggesting the functional heterogeneity of mast cells occurs (Prussin and Metcalfe, 2006). In addition, C2 mast cell line also synthesizes both PGD_2 and PGE_2 depending on stimuli (Mora et al., 2006).

2.3 Mast cell progenitor

Mast cells are derived from $CD34^+$ a multipotent hematopoietic precursor cell which is not a common myeloid progenitor in bone marrow (Hill and Martin, 1998). This cell linage commonly differentiates to give rise basophils and mast cells. These progenitor cells are influenced by various cytokines in a bone marrow microenvironment leading to the initialization of $CD34^+$ progenitor cell differentiation to produce mast cell offspring.

In vivo, mast cells do not circulate throughout the body as mature cells but in term of unidentifiable immature mast cell precursors (promastocytes). These cells then invade into and reside in their specific locations in tissues, such as the connective tissues and mucosal layer of gastrointestinal tracts to do differentiation and proliferation at the sites (Hill and Martin, 1998). In recent consensus, immature mast cell progenitors that circulate in blood expressing surface protein markers of KIT^{hi}/ $CD34^{+}$/ Thy-1^{lo}/ FcεRI^{lo} on their membranes. These marker expressions are quite different from mature mast cells (KIT^{hi}/ $CD34^{+}$/ FcεRI^{hi}). They are agranular or contain a less number of cytoplasmic granules which found abundantly in mature mast cells in their cytoplasm (Hill and Martin, 1998; Austen and Boyce, 2001; Mora et al., 2006). Moreover, mast cell progenitors express membrane aminopeptidase (CD13) but not CD14 on their membranes. The absence of CD14 expression is beneficial for distinguishing mast cell progenitors from monocytes (Austen and Boyce, 2001). It is noteworthy that mature mast cells might express monocyte/macrophage markers on their membranes, as well (Austen and Boyce, 2001). In human studies, four-weeks mast cell progenitors consistently express a monophasic profile of KIT^{lo}/ $CD13^{+}$/ $CD34^{+}$/ Thy-1^{lo}/ FcεRI^{lo}/ IL-3Rα^{+}/ Integrin-$\beta3^{-}$ on their membranes (Austen and Boyce, 2001). By 7-9 weeks, mast cell progenitors alter their surface protein expression with KIT^{lo}/ $CD13^{+}$/ $CD34^{+}$/ Thy-1^{lo}/ FcεRI^{lo}/ IL-3Rα^{-}/ Integrin-$\beta3^{+}$ including the absence of CD14 and CD16 (Austen and Boyce, 2001). This phenomenon suggests that the heterogeneity of mast cells early taken place since in promastocytes. Besides, mast cell progenitors are immunohistochemically stained for tryptase, chymase and chloroacetate. Toluindine blue staining is also positive in mast cell progenitors in this stage and increased in the older progenitors (Auten and Boyce, 2001).

2.4 Regulation of mast cell differentiation, maturation, homing and activation

Mast cell differentiation is triggered in a bone marrow under the influence of various cytokines. After differentiaton in bone marrow, they leave the bone marrow in immature form and circulate via blood stream, until they reach the residential sites throughout the body. After that, they mature in almost vascularized tissues at the homed sites. Proliferation and maturation are influenced depending upon SCF locally secreted from fibroblasts and endothelial cells into the extracellular milieus (Prussin and Metcalfe, 2006). IL-4 upregulates an FcεRI expression in mast cells, meanwhile

IL-5 in association with SCF can augment mast cell proliferation in their residential sites. IFN-γ has been reported to downregulate mast cell proliferation and maturation (Prussin and Metcalfe, 2006). Both of mast cell progenitor and mature mast cell possess large chemokine and adhesion molecules, which play the critical role in mast cell homing. Common adhesion molecules critically expressing for mast cell migration and homing are integrins, intercellular adhesion molecules 1 and 3 (ICAM-1 and ICAM-3), leukocyte function-associated antigen 1 and 3 (LFA 1 and LFA 3), CD44, transforming growth factor-β (TGF-β) and singlec-8 (Moldering, 2010). Recently, approximately 61 species of integrin have been defined in human mast cells which presumably resemblance in canine species.

In mouse studies, the results have substantially indicated that the mast cell homing in small intestines facilitated by a binding between $\alpha 4\beta 7$-integrin to mucosal address in cell adhesion molecule-1 (MAdCAM-1) or to vascular cell adhesion molecule-1 (VCAM-1). Meanwhile, for mast cell homing to the lung, the process recruits $\alpha 4\beta 7$- and $\alpha 4\beta 1$-integrins binding to VCAM-1 suggesting that mast cell homing is an organ-specific process (Moldering, 2010).

In general, an activation of mast cells in physiological and pathological responses is triggered through FcεRI on their cell membranes. However, other chemomediators and cytokines, such as C3a, C5a, IgG can also activate mast cells through each responsible receptor (C3aRI, C5aRI and FcγRI, respectively). Mast cells are also activated with toll-like receptor (TLR) especially TLR3 which promotes type 1-interferon production in mast cells (Prussin and Metcalfe, 2006). The activation of mast cells through IgE launches; when IgE bind to $\alpha\beta\gamma_2$ subunits of FcεRI on mast cell membranes. The activation of mast cells is influenced by three major factors; a signaling pathway, an intensity of signals and cytokines, particularly SCF.

2.5 Physiological and pathological functions of mast cells

Mast cells are thought to be the first responding cells to almost tissue injuries assaulting to the body. They usually accompany to the initial step of inflammatory process called early phase reaction (EPR) (Mora et al., 2006). The predominant role of mast cells in diseases has been described widely in many mast cell-dependent allergic disorders, such as allergic bronchitis and atopic dermatitis (AD), for instance.

Mast cells physiologically respond to the signals from both innate and acquired immunity. In innate immunity, mast cells can phagocytose bacteria (Prussin and Metcalfe, 2006). Mast cells also have the potential as the first immune cells responding to pathogens within several seconds via various pathogen recognition systems (Abraham and St. John, 2010). For example, mast cells contain toll-like Receptor- 2 (TLR-2) on their cell membranes which upregulate IL-4, IL-5, IL-6, IL-13 and TNF productions, while a TLR-4 promotes productions of IL-1β, IL-6, IL-13, and also TNF. Moreover, mast cells have an ability to replenish their granules with granular alterations after their degranulations leading to appropriate change in their morphologies and functions. This suggests that they contribute in reinfection controls. Recently, mast cells are also proposed to be beneficial or detrimental for tumor growths. For example, they can promote human mammary gland tumor development by disturbing communication between normal stroma and epithelium as well as they promote tumor angiogenesis or even release growth factors, such as nerve growth factor (NGF) or stem cell factor (SCF), leading to an excessive tumor growth (Conti et al., 2007). Mast cells are presently thought to contribute in pathological cardiovascular disorders, such as ventricular remodeling leading to severely excessive ventricular hypertrophy via extrarenal renin production by cardiac mast cells juxtaposed to the nerve endings in ventricles (Silver et al., 2004; Mackins et al., 2006; Kaesnikoff and Galli, 2008). In addition, mast cells also reportedly contribute in wound healing, angiogenesis, fibrosis and chronic inflammatory processes (Hill and Martin, 1998). Hence, it is necessarily needed for further study for fully understanding of the functional diversity of these enigmatic cells.

2.6 Mast cell identifications

According to mast cells contain in many of physiological cytoplasmic granules accompanying to various conditions especially in innate and acquired immune responses. Histologically, mast cells are not easily diagnosed with a conventional hematoxylin and eosin (H&E) stain. From time to time, they might be resemblance to other cell populations, such as fibroblasts, histiocytes and monocytoid-B cells. In this case the other staining systems such as wright-giemsa and toluidine blue are very useful to distinguish mast cells from the others. Wright-giemsa stain can demonstrate distinct basophilic cytoplasmic granules in mast cells meanwhile toluidine blue stain confirms metachromatic property of cytoplasmic granules. However, the metachromatic granules

could be diminished with the conventionally histological tissue process particularly when acidic solution is used. The immunocytochemistry of chloroacetate esterase and aminocaproate esterase are also reportedly helpful to classify mast cells from other mimic cells, because mast cells in general are rich of these two enzymes. However, chloroacetate esterase is also found in neutrophillic myelocytes, meanwhile aminocaproate esterse albeit is more specific for identifying mast cells but it is also required a special tissue processing protocol (Li et al., 2001).

Since tryptase- and CD117-immunohistochemistry have been introduced to pathologists, these two methods are beneficial for an identification of normal and neoplastic mast cells (Li et al., 2001; Morini et al., 2004; Kiupel et al., 2004). However, abnormal basophils in some circumstances could be positively reactivated by tryptase-immnunohistochemistry. Even basophils are negative with CD117-immunohistochemistry; however, CD34-positive myeloid precursor cells are weak positive to CD117-immunohistochemistry as well. Moreover, a small subset of small lymphocytes presumably NK cells are also significantly positive to CD117-immunohistochemistry (Li, 2001). The summary of cytochemical and immunohistochemical protocols employed to classify mast cells is present in Table 2.1.

Table 2.1 Commom cytochemical and immunohistochemical characteristics in mast cells (modified from Li, 2001).

	Mast cells	Basophils	Promyelocytes	Megakaryocytes	Granular Lymphocytes
Peroxidase	-	-	+ + + +	-	-
Toluidine blue	+ + + +	+ + +	-	-	-
Chloroacetate esterase	+ + + +	-	+ + +	-	-
Aminocaproate esterase	+ + +	-	-	-	-
Tartrate-resistant acid phosphatase	+	-	-	-	-
Tryptase	+ + + +	+/-	-	-	-
CD41	-	-	-	+ + + +	-
CD56	-	-	-	-	+/-
CD117	+ + + +	-	-	-	+/-

2.7 Flow Cytometry applications for mast cell studies

The usage of flow cytometry (FCM) in a classification of mast cells has been previously described in several literatures in human counterparts. For example, FCM was applied in a cell sorting to separate circulating mast cell progenitors from the human bone marrow. The FCM-cell sorting in that study was performed based upon the differently phenotypic properties of these rare progenitor cells on their membranes to other hematopoietic precursor cells. Because these progenitor cells express KIT^{hi}/ $CD34^{+}$/ $Thy\text{-}1^{lo}$/ $Fc\varepsilon Ri^{lo}$ with a few fine cytoplasmic granules. The Anti-human antibobies for those surface molecules were employed to distinguish mast cell progenitors from other marrow hemopoietic cells. The group of mast cell progenitors was gated and then collected by flow cytometry cell sorting in this study. In addition, FCM could also facilitate for study mast cell progenitor granularity using the side angle light scattering pattern (SSC) parameter, in this study. The result substantially exhibited that four-week-old mast cell progenitors had a low SSC in the meantime this property was increased in older progenitors. It indicated that older progenitors contain more cytoplasmic granules than in younger mast cell progenitors (Austen and Boyce, 2001).

With a highly sensitive and specific property of flow cytometry (FCM) in an analysis of multiple parameters of individual cells in a cell suspension and more species-specific antibodies with species cross-reactivity of antibodies is recently determined; FCM is to date increasingly used in veterinary medicine, as well. In veterinary oncology, the utilization of FCM is for study of immunophenotyping to assess the expression of cell markers and for determination of the DNA content of cells with fluorescent dyes that bind nucleic acids (Reggeti and Bienzle, 2011). Moreover, flow cytometry is enabled for a rapid analysis of multiple cellular parameters of discrete cells such as cell size, cytoplasmic complexity, DNA-ploidy, RNA content, membrane-bound and intracellular proteins (Culmsee and Nolte, 2002). For instance, in one study of mast cell leukemia, the peripheral blood of the case was analyzed with MAPSS^{TM} flow cytometric technique. The size and complexity scattering patterns were plotted. The result has shown that the averaged size of mast cells in this case was nearly equal to the monocyte while the granularity of mast cells was resemblance to basophils (Prihirunkij et al., 2007). This result has been clearly emphasized the application of FCM for distinguishing mast cells from other cells in the peripheral blood.

2.8 Canine cutaneous mast cell tumors

MCT is a common cutaneous tumor in dogs thought to be arisen from the abnormal proliferation of mast cells in the skins. Recently, the exact tumorigenesis of MCT is not well established. MCT is usually seen in dogs aging more than 8 year-old with no gender predilection. For breed predilection, it is arguably however Boxer, Bull dog, Pug, Labrador retriever, and Golden retriever have been accounted for the most susceptible breeds for MCT. The gross appearance of MCT usually resembles to other cutaneous tumors in dogs. It usually shows up as a pinkish-solitary mass, with or without ulceration on the skins and subcutaneous tissues. From time to time, MCT is quite hardly distinguished from other skin tumors. Moreover, Golden retrievers frequently have multiple tumors but they are not necessarily associated with the poor prognosis. The tumor site is also significantly, in particular of MCT on mucocutaneous junctions such as buccal cavities and inguinal areas, these MCT are more aggressive than those found on the skins. The metastatic MCT is rarely found in dogs with the low incidence of 3% in the MCT population (Dobson and Scase, 2007).

In general, almost clinical presentations of MCT are solitary, well circumscribed, raised and firm nodules on skins. However, 10% to 15% of MCT dogs present multiple tumors, as well. The most frequently preferential sites are 50% on the trunks and perineal regions, 40% on the limbs, and 10% on the heads and necks. A tumor mass might be erythematous and ulcerated in some circumstances. A deep invasion into the underlying subcutaneous tissues might be observed in some patients with poorly circumscribed mass in subcutis which resemble to lipomas. Basically, benign MCT grows very slowly but in somehow many malignant MCT grow very rapidly of which always come along with poor prognosis in almost cases (London and Seguin, 2003).

Clinical signs of MCT in general are caused by the release of histamine, heparin and other vasoactive amines contained in membrane-bound cytoplamic granules of MCT cells. Interestingly, a mechanical manipulation of the tumor during physical examination can induce degranulation leading to severe erythema and wheal formation which usually called Darrier's sign in MCT dogs. The other seriously paraneoplastic syndrome is gastrointestinal ulceration which is account for 35% to 83% of MCT dogs undergone necropsy. Clinicopathologically, plasma histamine concentrations are usually shifted in almost MCT dogs which presumably affecting to H2 receptors

on parietal cells of stomachs. The stimulation on H2 receptors causes the excessive production of gastric acids resulting in the development of gastric ulcers. Anyway, the increased levels of histamine has been reported not to be related to clinical stage, histopathologic grade or even tumor size (London and Seguin, 2003; Thamm and Vail, 2007).

2.9 The proto-oncogene *c-kit* and mutations

As aforementioned above, the exact tumorigenesis of MCT is not well established. However, from previous studies showing that the proto-oncogene *c-kit* has been reported to contribute in the MCT pathogenesis (London et al., 1999; Letard et al., 2008). This proto-oncogene encodes the transmembrane type III-receptor tyrosine kinase (Type III-RTK), KIT protein, in mast cells (Letard et al., 2008). Since the proto-oncogene *v-kit* had been identified and described in feline sarcoma caused by Hardy-Zuckerman 4-feline sarcoma virus in domestic cats in 1986 (Edling and Hallberg, 2007). The proto-oncogene *c-kit* was also studied and sequenced. The consequence has shown that the DNA sequence of this proto-oncogene is similar to *v-kit*. Moreover, *c-kit* is highly conserved among mammals. For example, canine *c-kit* is 88% and 82% homology to human and mouse *c-kit*, respectively (London et al., 1999).

In general, the exons dictating the KIT formation in *c-kit* consists of exon-1 to 21. Each exon functionally involves in the generation of individual portion of KIT. Therefore, every mutations in these exons results in a perturbation of KIT formation leading to an uncontrollable proliferation of mast cells, finally causing MCT genesis (London et al., 1999; Letard et al., 2008). The most frequently genetic alteration of exons has been reportedly seen in exon-11 of *c-kit* (Zemke et al., 2001; Letard et al., 2008). Besides, canine exon-11 is 100% compatible to exon-11 in human and mouse (London et al., 1999). Moreover, the mutations of exon-8, 9 and 17 have been officially reported as well (Letard et al., 2008).

The frequent mutation of exon-11 is 45 to 70-base-paired duplication ($ITD^{571-590}$) at the distal part (3' end) of exon-11 in MCT cells. The other mutant subtypes which rarely seen are at the proximal portion (5' end) of exon-11 are point mutations, insertions, in-frame mutations and deletions; such as $Del^{555-557}$ InsV, $Del^{556-557}$, K^{557} InsF, K^{557}N InsP and K^{557}R $Del^{558-559}$ (London et al., 1999; Zemke et al., 2001; Zemke et al., 2002; Letard et al., 2008). Nevertheless, the duplicated

mutation in exon-11 has also been defined in C2-MCT cell line (Zemke et al., 2001). Albeit, the poly-T insertion in intron-12 has been discovered in MCT cells; however, it has no mean in MCT pathogenesis because it is the non-coding region (Zemke et al., 2002). Furthermore, there is no report for exon-mutations in *c-kit* which controlling the formation of tyrosine kinase domain in KIT, so far (Dobson and Scase, 2007). The common exon mutations are summarized in Table 2.2.

Table 2.2 Usual exon mutations frequently observed in canine cutaneous mast cell tumors (modified from Letard et al., 2008)

Mutant Exon	Mutation Category	Equivalent Residues in Human KIT	No of Dogs (% of Total)
Exon 8	$ITD^{417-421}$	418	8
	$Q^{430}R$	427	1
	Total	-	9 (4.7%)
Exon 9	$S^{479}I$	476	5
	$N^{508}I$	505	3
	Total	-	8 (4.2%)
Exon 11	$Del^{555-557}InsV$	556-558	1
	$Del^{556-557}$	556	1
	$K^{557}InsF$	558	1
	$K^{557}N$ InsP	558	3
	$K^{557}R$ $Del^{558-559}$	558	1
	$ITD^{571-579}$	573-581	1
	$ITD^{571-581}$	573-583	1
	$ITD^{571-583}$	573-585	2
	$ITD^{571-585}$	573-587	1
	$ITD^{571-589}$	573-591	2
	$ITD^{572-583}$	574-585	1
	$ITD^{572-585}$	574-587	1
	$ITD^{572-586}$	574-588	2
	$ITD^{572-587}$	574-589	1
	$ITD^{572-588}$	574-590	4
	$ITD^{572-589}$	574-591	1
	$ITD^{572-590}$	574-592	1
	$ITD^{573-585}$	575-587	1
	$ITD^{573-590}$	575-592	1
	$ITD^{573-591}$	575-593	1
	$ITD^{575-582}$	577-584	1
	$ITD^{576-590}$	578-592	3
	Total	-	32 (16.8%)
Exon 17	$Del^{826-828}$ InsDT	827	1 (0.5%)
All mutations		-	50 (26.2%)

The incidence of exon-11 mutation in *c-kit* has been reported varying from 9-33 % in MCT biopsied specimens (Downing et al., 2002; Zemke et al., 2002; Webster et al., 2006; Letard et al., 2008) as well as in C1 and C2 cell lines (Ma et al., 1999; Downing et al., 2002). This information might indicate that there might be other mutated genes involving in MCT tumorigenesis.

2.10 Evaluation of exon-11 mutation in *c-kit*

Traditionally, most exon-11 mutations in *c-kit* have been studied using standard polymerase chain reaction (PCR) method. The consequences from former studies have consistently shown 45 to 70-bp internal tandem duplication (ITD) in the mutated exon-11. Usually, the PCR products have been analyzed by standard gel electrophoresis which showing 3 bands of 191-bp heterogenous normal allele, 250-bp mutated allele and the heterodimerization (heteroduplex) strip. The heteroduplex is formed due to the complementary nucleotides of normal and mutant alleles have annealed together (Zemke et al., 2002; Webster et al., 2006).

In the previous study, the result has implicated that MCT patients with exon-11 ITD-mutation in *c-kit* associated with aberrant KIT localization in MCT-grade II and III had worse prognosis when compared with MCT-grade I patients (Zemke et al., 2002). Despite *c-kit* is responsible for the mast cell development and survival (Zemke et al., 2001); therefore, a mutation of any exons in *c-kit* may associate in MCT tumorogenesis at least in promoting of uncontrollable proliferation of MCT cells without any specific ligand bindings.

2.11 Molecular structure of KIT and its signaling pathway

KIT is a 145 kDa glycoprotein. It is a member of type III-receptor tyrosine kinase. The other well-known receptors in this class are platelet derived growth factor-α and -β (PDGF-α and -β), macrophage-colony stimulating factor-1 (CSF-1, M-CSF or FMS) and Flt-3 receptor (FLK2). Normally, KIT is tremendously express in hematopoietic precursor cells in the bone marrow; however, the expression of KIT is downregulated in almost cells except in mast cells after maturation. Moreover, several such non-hematopoietic cells and tumors also express KIT on their membranes (Hubbard and Till, 2000; Edling and Hallberg, 2007).

The structure of KIT composes of three principal domains; the glycosylated extracellular (Ectodomain), transmembrane (TM) and intracellular domains which encoded by exon-1 to 9, -10 and -11 to 21, orderly (Roskoski, 2005; Edling and Hallberg, 2007; Yuzawa et al., 2007; Letard et al., 2008). The specific ligand for KIT is normally known as stem cell factor (SCF). The alternative synonyms of this ligand are mast cell growth factor (MGF), KIT-ligand, p145 and Steel Factor.

The extracellular domain consists of five immunoglobulin-like repeating units designed as D1, D2, D3, D4 and D5. These motifs are members of the immunoglobulin super family (IgSF). D1, D2, D3 and D4 belong to I-subset meanwhile D5 is a member of C2 and IgCAM subsets of IgSF. Each repeating unit composes of eight β-pleated sheet polypeptides (designed as ABCC'DEFG) arranging in an anti-parallel conformation. D1 and D3 contain single disulfide bond meanwhile D2 and D5 form two disulfide bonds in each domain. These disulfide bonds link to cysteine residue in the domain to hold each domain together. Interestingly, D4 does not contain a cysteine residue in the domain based on molecular X-ray diffracted crystallography study.

The ectodomain topology is also stabilized by hydrophobic and electrostatic forces between amino acid residues in β-sheet of one subunit to its neighboring subunits, except D4-D5 interface is maintained by hydrophobic interaction only. Nevertheless, the D1-D2 interface which containing many amino acid residues in the strand G of D1have been found that the linker region which connecting D1 and D2, and the BC loop of D2 are conserved in different species. The signal sequence is in the N-terminal of ectodomain (Edling and Hallberg, 2007). The function of ectodomain is primarily providing a binding site to SCF. To achieve this function, D1, D2 and D3 constitute a concave pocket which interfacing exclusively to SCF (Edling and hallberg, 2007; Yuzawa et al., 2007).

The transmembrane domain of KIT is the short hydrophobic polypeptide penetrating into the cell membrane. This portion acts as the anchoring protein to fix KIT on cell membranes. The intracellular or cytoplasmic domain contains two moieties; juxtamembrane as the negative regulator (autoinhibitor) for KIT signaling (Edling and Hallberg, 2007) and the cytoplasmic tyrosine kinase. The juxtamembrane and cytoplasmic tyrosine kinase are separated by the ATP-

binding sites and phosphotransferase lobes which encoded by exon-13 and 17, respectively (Letard et al., 2008). The tyrosine kinase motif could be further divided into the distal and proximal parts of which separated by a variable in length-insertion motif. Apart from distal kinase motif, there is the activation loop situates in this region (Edling and Hallberg, 2007).

Physiologically, the specific ligand for KIT is stem cell factor which induces autophosphorylation to tyrosine residues on juxtamembrane domain, tyrosine kinase domain and C-terminal of KIT after the ligand binding (Hubbard and Till, 2000). The biological function of KIT is to promote the development of mast cells from hematopoietic progenitors in bone marrow in association with a number of cytokines leading to the increased rate of mast cells entering to the cell cycle (Webster et al., 2007); as well as, it control proliferation and survival of mast cells. Therefore, it is essential to comprehend the basis of normal KIT signaling pathway before applying this information in an explanation of the role of mutant KIT in MCT-pathophysiology.

Basically, the activation of KIT and its signaling is attained depending on two related processes; an augmentation of intrinsic catalytic pathway at the catalytic domain of KIT and a creation of binding sites for downstream signaling molecules (Hubbard and Till, 2000), and what's up after the activation? The non-covalent dimerization of KIT will lead to a structural rearrangement of KIT providing the binding sites for additional signaling proteins which facilitating the cytoplasmic domains to generate autophosphorylation. This suggests that a monomeric KIT exerting as an enzyme and a substrate to each other KIT in autophosphorylation.

After the ligand binding, the orphan (monomeric) KIT forms the ligand-receptor dimer complex in the ratio of 2 SCF: 2 KIT molecules leading to an initiation of autophosphorylation of tyrosine residues on KIT themselves followed by the downstream cascade of KIT signaling (Hubbard and Till, 2000; Edling and Hallberg, 2007). Autophosphorylation of the activation loop in tyrosine kinase domain causes the stimulation of tyrosine kinase activity followed by autophosphorylation of juxtamembane domain, tyrosine kinase insert and C-terminus. The phosphotyrosine in these three regions provide the docking sites for the downstream signaling molecules in KIT (Hubbard and Till, 2000).

The downstream cascade of KIT signaling pathway is followed the phosphorylation on various secondary messengers and other signaling protein kinases, such as non-receptor protein kinases (NRTK) and transcription factors by phosphotyrosines when binding to their corresponding docking sites (Hubbard and Till, 2000). These activated signaling molecules then accompany into the signaling pathways of KIT. The consequence of KIT signaling involve in the control of mast cell differentiation, development, proliferation, biochemical alteration and migration. The important attribute of downstream signaling proteins is they must contain two crucial domains on their molecules; phosphotyrosine-binding domain (PTB) and SH2 domain. Moreover, the cytoplasmic domain of KIT also stabilizes transiently for KIT dimerization after autophosphorylation (Hubbard and Till, 2000).

As in FcεRI-induced mast cell activation, the mitogen-activated protein kinase (MAPK) is activated after KIT dimerization causing MAPK-dependent signaling cascade activation. For instance, Mek and the extracellular signal-regulated kinase, Erk are stimulated by Ras-GTPase resulting in a relocation of Erk into the nucleus of mast cells. Relocated Erk then phosphorylates various transcriptional factors (TF) which initiate a gene transcription essential for mast cell development and proliferation. PI-3 is another kinase which activated by KIT dimerization. The activation of PI-3 will recruit protein kinase-B (PKB or Akt) onto cytoplasmic membranes of mast cells, where PKB is activated leading to anti-apoptotic effect to mast cells. Moreover, PI-3 signaling pathway also participates in stem cell renewal and a regulation of many mast cell functions. The ligand binding-dependent dimerization of KIT also activates small GTPase, Rac which will stimulate c-Jun transcription factor and PKB. The activation would affect on proliferation, development and degranulation of mast cells. Raf activation is also independently activated with PI-3 after dimerization.

KIT signaling pathway is regulated via several mechanisms. KIT degradation is the most common pathway used for modulating the KIT signal. KIT is decayed via Cbl, an E3 ubiquitin-protein ligase, which promotes the KIT decomposition via a proteasome or lysosome. Moreover, the kinase activity of KIT is also downregulated by a SH2 domain-containing phosphatase-1, Shp1. This molecule is a cytosolic phosphotyrosyl phophatase which binds to Y570 residue in KIT or other KIT-associated tyrosine kinases resulting in subsequently dephosphorylation of those phosphorylated tyrosine kinases. Protein kinase C (PKC) also deactivates KIT signaling pathway by phosphorylating

on specific serine residues in KIT causing the negative feedback loop regulating the KIT activation (Edling and Hallberg, 2007).

2.12 Juxtamembrane domain of KIT in MCT-Pathophysiology

Very recently, juxtamembrane mutations have been reportedly involved in the development of MCT. Spontaneous tyrosine autophosphorylation of KIT ensued by juxtamembrane mutations leads to an intrinsic inhibitory constraint of KIT signaling. Recent studies have exhibited that juxtamembrane domain of normal KIT forms a V-shaped loop inserting into the interface between the small and large lobes of the kinase domains. In the autoinhibited state of KIT, the hydroxyl group of Tyr823 in juxtamembrane domain of inactive KIT forms a hydrogen bond with the catalytic Asp792 thereby preventing the binding of protein substrates to the activation site. In addition, Phe811 of the DFG segment also prevents the binding of the adenine of ADP to the docking sites. Moreover, kinase inhibitions by juxtamembrane domains also take place by displacing the αC-helix of kinase domain. This displacement prevents the activation loop extension and the movement of the small and large lobes of kinase domains which necessary for the binding and releasing of substrates (Roskoski, 2005). Biochemically, the replacement of the amphipathic residue Trp at the position 556 of KIT with Arg is the causative factor for the autoactivation of KIT (gain-of-function). This replacement suggests that the hydrophobic side chain of Trp is important for the inhibition of KIT signaling. In addition, the deletions of Trp556–Lys557 or Val558 as well as the substitution of Pro for Leu575 have similar effects to Trp replacement.

2.13 Diagnosis of canine cutaneous mast cell tumors

Nowadays, the accurate diagnosis and prognosis workup for MCT is based on various parameters depending on the systems acquired by veterinary pathologists and veterinary oncologists. So far, there is no single parameter can diagnose and prognosticate MCT accurately in one step. Basically, MCT diagnosis is performed based on various histopathological parameters such as cellular differentiation, mitotic rate and tumor invasion. These parameters may be helpful for predicting a tumor biological behavior, grading and prognosis, in some circumstances (Welle et al. 2008). Nowadays, there are two histopathological grading systems commonly used for MCT diagnosis issued by Bostock and colleagues in 1973 and Patnaik et al. in 1984, respectively. However, Patnaik histopathologic grading system seems to be the most favorite tool used by almost

veterinary pathologists for MCT grading. The schematic grading criteria in both systems are grounded a cellular and nuclear morphology, cellularity of neoplastic cells, cellular differentiation and mitotic index (Bostock et al., 1973; Patnaik et al., 1984). However, each histopathological grade in Patnaik grading system is also found on tumor invasiveness and depth (Patnaik et al., 1984) meanwhile the nucleus and cytoplasm ratio is used in Bostock histopathologic grading system (Bostock et al., 1973). Both grading systems score each MCT into 3 distinct grades; grade I, II and III, respectively. It is noteworthy that these two MCT grading systems distinguish MCT in the inverse order, from each other. For example, MCT-grade I (well-differentiated) and –grade III (undifferentiated) in Patnaik grading system are MCT-grade III and -grade I in Bostock grading system, respectively, meanwhile MCT-grade II is consistently resemble in both grading systems (Thamm and Vail, 2007). Both grading systems also provide a prognostic parameter for MCT using the association between each MCT-grade to survival time. A well-differentiated MCT always has a prolong survival when compared with undifferentiated MCT (Bostock et al., 1973; Patnaik et al., 1984; Thamm and Vail, 2007). Recently, a novel MCT-histopathologic grading system has been introduced into the veterinary pathology field. This 2-tier histopathologic grading divided MCT into 2 classes, low-grade and high-grade MCT based on these criteria, at least 7 mitotic figures in 10 high power field (HPF), more than 3 multinucleated neoplastic cells in 10 HPF, at least 3 bizarre nuclei or 2-fold karyomegaly in 10 HPF. Once MCT is fitted into one of these criteria, it is classified into high-grade MCT. This novel grading system has improved the concordance among veterinary pathologists in MCT grading when compared to Patniak histopathologic grading systems. Moreover, the association between histopathologic grades and survival time is also seemingly predicted more precisely than in Patniak MCT-histopathologic grading systems as shown in Figure 2.1 (Kiupel et al., 2011).

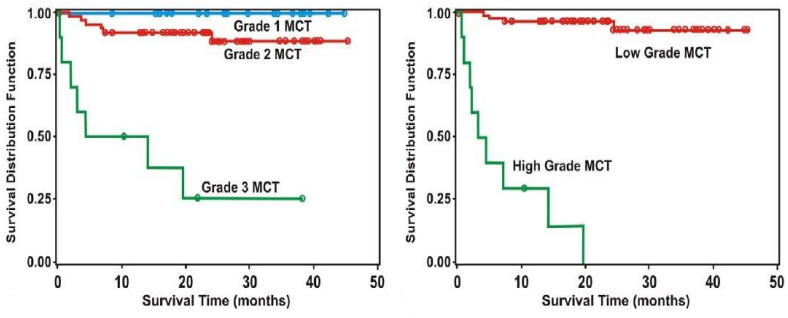

Figure 2.1 The comparative result of the correlation of each histopathologic grade to its corresponding survival time in Patniak histopathologic grading system (on the left) compared with the novel 2-tier histopathologic grading system (on the right).

In addition, the other parameters reportedly used for MCT diagnosis, grading and prognosis to date are clinical stage, tumor location, breed, growth rate/duration, PCNA, tumor recurrence, AgNOR count and intratumoral vessel density (Dank 2005).

Metastatic MCT even rarely taking place, however MCT dogs with metastasis are required a lymph node and bone marrow investigation, as well as an evaluation of a buffy coat of whole blood to figure out mastocytemia, even though not all metastatic MCT dogs have mastocytemia (Dobson and Scase, 2007; Prihirunkij et al., 2007). Fine-needle aspiration (FNA) is also the best useful screening tool for veterinary pathologists and veterinary clinicians to quickly initiate a diagnostic workup. However, with the limitation of this tool is therefore it could not properly identify bad grade II or high-grade MCT cells in many cases, because these MCT-cells morphologically resemble to other round cell tumor cells, especially, TVT and histiocytomas. Therefore, in this case, a specific stain such as toluidine blue is essential to be used for distinguishing them from other round cell tumors (Prihirunkij et al., 2007). Previously, various cellular parameters such as tumor growth rate and cell generation time which used for determining a prognosis for MCT, have been also employed for MCT diagnosis and prognosis. Generally, the tumor growth rate is proportionate to generation time and growth fraction of tumor cells, meanwhile proliferation is inversely proportionate to the generation time associated with growth fraction (Zemke et al., 2002). There have been many investigators using the proper markers to identify these parameters for tumor prognosis. The parameters have been commonly used are argyrophillic nuclear organizing region proteins (AgNORs), proliferating cell nuclear antigen (PCNA), and Ki-67. AgNORs is useful for determination of nuclear generation time but it does not determine the phase of the cell cycle, meanwhile PCNA and Ki-67 have been used for indicating a number of actively proliferating tumor cells on various phases of the cell cycle (Newman et al., 2007). However, Ki-67 is seemed to be a highly independent prognostic marker for MCT when compared with the others (Dobson and Scase, 2007; Webster et al., 2007).

Recently, CD117-immunohistochemistry is applied for study a localization of KIT in both normal and MCT tissues including normal skin mast cells (Kiupel et al., 2004; Morini et al., 2004; Gil da Costa et al., 2007). There are three staining patterns found in CD117-immunohistochemistry. In pattern I, the CD117-immunoreactivity is prominently on the plasma membranes of MCT cells

(perimembrane pattern). For the staining pattern II, the CD117-immunopositivity consistently focally aggregates in cytoplasm adjacent to the nuclei of neoplastic cells (paranuclear pattern). The staining pattern III is found the immunoexpressions of CD117 diffusively distribute throughout the cytoplasm of tumor cells. This pattern is called the cytoplasmic diffuse pattern (Kiupel et al., 2004; Gil da Costa et al., 2007). The results from previous studies has substantially shown that the role of different staining patterns is very important, because the perimembrane pattern is usually not associated with local or distant metastasis of MCT, or even not associated with survival time, while the others do (Kiupel et al., 2004). In addition, CD117-immunocytochemistry has been reportedly utilized in study of KIT localization in FNA-MCT cells, as well. From one previous study, the result has substantially exhibited that there were three distinguished CD117-immunolabeling patterns identified which compatible to those decribed in CD117-immunohistochemistry (Theerawatanasirikul et al., 2009).

To date, the standard PCR can potentially be used in the study of exon mutations in *c-kit* in MCT cells. However, most of the MCT cells used in previous studies were obtained from biopsy; hence, there is no evidence in a use of standard PCR to study MCT cells obtained by FNA method has been reported, so far. RT-PCR is also a sensitive tool for study kinetic activity by quantitative determination level of mRNA on *c-kit* expression both in MCT cells and tissues. Both of mutated exon in *c-kit* and increased mRNA level of *c-kit* have substantially related to the poor prognosis for bad grade II and grade III MCT patients suggesting that these two parameters might have a prognostic value for MCT patients as well as for a therapeutic intriguing (Turin et al., 2006; Webster et al., 2006).

Exon mutations in c-*kit* recently reported are point mutation, deletion, and duplication. Most of mutation is found in exon-11 which encoding for juxtamembrane domain of KIT and intron-11 mutation in *c-kit*, both in MCT cells and mast cell lines (Zemke et al., 2001). To date, the acceptable proto-oncogene *c-kit* mutation in canine MCT that naturally found is the 45 to 70-bp insertion at 3' end of exon-11, and poly-T insertion in intron-12 (London et al., 1999; Zemke et al., 2002). However, there is no report for kinase domain mutation in KIT, so far (Dobson and Scase, 2007). The incidence of ITD mutation of exon-11 in *c-kit* has been reported to vary from 9-33 % in MCT biopsied specimens (Downing et al., 2002; Zemke et al., 2002; Webster et al., 2006) as well as in C1 and C2 cell lines (Ma et al., 1999; Downing et al., 2002), indicating that there might be other

mutated genes involving in MCT tumorigenesis. Traditionally, exon-11 mutation in *c-kit* has been studied using PCR. The consequences from those studies have consistently shown 45 to 70-bp ITD in mutated *c-kit* with 3 bands of 191-bp heterogenous normal allele, 250-bp mutated allele, and the heterodimerization or heteroduplex between normal and mutant alleles, if any, as the largest fragments (Zemke et al., 2002). From a previous study has also shown that MCT patients with ITD mutation of exon-11 in *c-kit* associated with aberrant KIT localization in MCT-grade II and III) had worse prognosis when compared with MCT-grade I patients (Zemke et al., 2002).

2.14 Canine cutaneous mast cell tumors therapy

The therapeutic strategy for all MCT patients is based on the histopathologic grading. However, it is highly questionable especially in the intermediate-grade MCT, what is an appropriate therapeutic protocol suitable for this grade? The most effective conventional therapies for MCT dogs are a surgically removal with widely excision from the tumor margins (at least 2-3 inches in three-dimension) and chemotherapy, such as vinblastin, vincristine, cyclophosphamide, and prednisolone. However, radiotherapy is also a useful therapy of choice especially in case of unresectable MCT. Furthermore, chemotherapy is also used in a treatment of disseminated, non-resectable or high-grade MCT especially when a radiation therapy is unfeasible (Welle et al., 2008). Recently, there are many chemotherapeutic drugs and protocols have been devised and introduced for MCT therapy. Each chemotherapeutic agent might be used as a single therapeutic agent or in a combined chemotherapy. For example, vinblastine might be used alone or combined with several chemotherapeutic agents such as prednisolone and cyclophosphamide to augment its therapeutic efficacy on MCT.

Although, the exact mode of action of corticosteroids; such as prednisone and prednisolone, in the treatment of MCT is not really known. However, there has been report showing that at least 20% of MCT dogs respond to corticosteroid therapy. The remission time of MCT in prednisone monotherapy is approximately 10 to 20 weeks. Intralesional corticosteroids have also been shown some benefits for MCT therapy (London and Seguin, 2003). CCNU, a nitrosourea alkylating agent, is also the one of good chemotherapeutic agents beneficial for MCT. Approximately 42% to 79% of MCT-grade II and III dogs respond to CCNU monotherapy (London and Seguin, 2003; Welle et al., 2008).

Vinblastine has been shown the efficacy against MCT, as well. One study in MCT dogs with lymph node involvements and distant metastasis, the MCT dogs had been administered prednisone at the dosage of 1 mg/kg P.O. daily for 2 weeks followed by 0.5 mg/kg daily with vinblastine at 2 mg/m^2, I.V. weekly for 4 weeks (Govier, 2003). The result has revealed that the combination protocol of vinblastine with prednisone effectively increased the median survival time of those MCT patients. These MCT patients had a mean survival time of 331 days. 45% of MCT patients were alive in more than 1 year (Govier, 2003; London and Seguin, 2003). Interestingly, a close relative of vinblastine; vincristine, apparently has a little efficacy in MCT treatment (London and Seguin, 2003). A combination of predinisolone and vinblastin is also an effective therapeutic protocol for MCT. In one study of 30 MCT dogs, the result has shown that the dogs undertaken the treatment with vinblastine sulfate and oral prednisolone exhibited in a decreased histopathological malignancy parameters, particularly AgNORs, PCNA, and Ki-67 indices including an increase of other clinical prognosis parameters, such as disease-free interval (DFI) and overall survival time (OS) when administered this combined chemotherapy to the dogs after surgery (Webster et al., 2008; Rungsipipat et al., 2009). Interestingly, high-grade MCT dogs with an aberrant KIT localization or increased Ki-67 and AgNORs values always respond to this combined therapeutic protocol very well when compared with the dogs treated by surgical removal only (Webster et al., 2008).

Recently, novel targeted-chemotherapeutic agents particularly tyrosine kinase inhibitors (TKIs), such as Gleevec™ (Imatinib), Kinavet™ (Masitinib) and Palladia™ (Toceranib) have been introduced into the field of veterinary oncology (Pryer et al., 2003; Dobson and Scase, 2007; London, 2009; Yancey et al., 2009). In particular Toceranib, the first approved TKI is used for MCT treatment in canine species. As known in above description that mutation of exon-11 in *c-kit* results in the constitutive autophosphorylation of KIT in MCT cells. The gain-of-function of KIT caused by exon-11 mutation leads to an aberrant intracellular signaling of KIT in MCT cells, presumably promoting an uncontrollable proliferation of MCT cells. Hence, any small molecule which can bind to tyrosine residues aligned in intracytoplasmic domains of KIT might promise a targeted chemotherapy to MCT patients (Dobson and Scase, 2007). These small molecules in general block ATP binding sites of juxtamembrane domain of KIT leading to the inhibition of phosphorylation to tyrosine residues and further hindering a signaling cascade which essential for control the cell growth and proliferation (London, 2009). Nevertheless, MCT dogs with mutant exon-11 in *c-kit* usually respond two-fold in TKI therapy, especially when Toceranib is in use, than in dogs whose do not contain mutant exon-11 (London et al., 2009).

CHAPTER III

MATERIALS AND METHODS

3.1 The conceptual framework

The research was run under this conceptual framework shown in Figure 3.1.

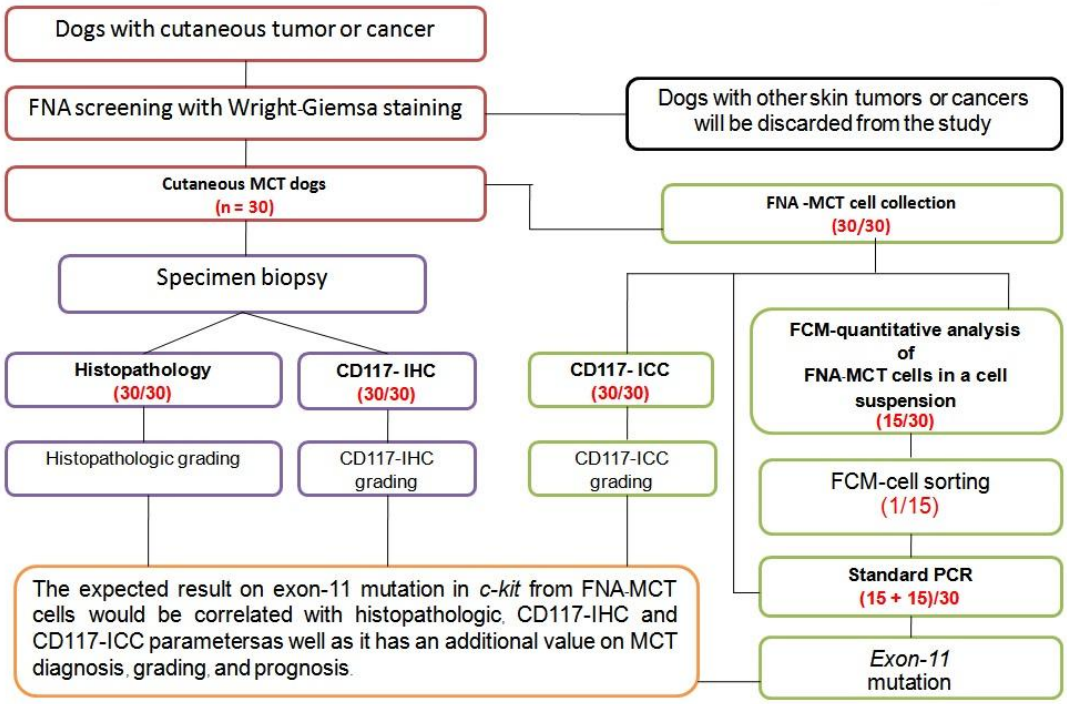

Figure 3.1 The conceptual framework used in this study

3.2 The tumor specimens

Dogs with all kinds of cutaneous masses were accepted into the Oncology Unit, Small Animal Teaching Hospital, Faculty of Veterinary Science, Chulalongkorn University during 2010 to 2012. The screening diagnosis using fine-needle aspiration (FNA) with giemsa staining system was done in each case. Non-MCT dogs were excluded from the study based upon the screening diagnosis. Thirty MCT dogs ratified by FNA-screening test were selected in the study with the completely individual information for anamnesis, clinical diagnosis, histopathologic diagnosis and

therapeutic protocols including the client conscience. TNM and clinical stage parameters for MCT diagnosis were not applied in the case selection.

3.3 Specimen collection for histopathology and CD117-immunohistochemistry

Each MCT dog was locally anesthetized with 1% Lidocaine HCl for a pain remedy. Afterward, each MCT dog was biopsied for collecting a tissue sample. The biopsied specimen was preserved in 10% buffered formalin solution for 5 days before performing tissue processing. The biopsied specimens were then submitted to the Pathology Unit, Department of Veterinary Pathology, Faculty of Veterinary Science, Chulalongkorn University for tissue processing. The final histopathological diagnosis and grading were defined by a qualified veterinary pathologist and the author using Patnaik histopathologic grading system for MCT (Patnaik et al., 1984). Ultimately, each MCT dog was classified into MCT-grade I, -grade II and -grade III groups respectively, based upon its corresponding histopathological grade.

3.4 Tissue processing for histopathology and CD117-immunohistochemistry

The formalin-fixed biopsy specimen was treated using the standard protocol recommended by the Pathology Unit, Department of Pathology, Faculty of Veterinary Science, Chulalongkorn University. The preserved specimen was cubically trimmed in the dimension of 2x2x2 cm^3. Afterward, the tissue specimen was embedded in a paraffin block using the automatic tissue processing machine. Each paraffinized specimen was sectioned by a microtome at 4 μm thickness. The sectioned specimen was relocated onto a glass slide and immersed in xylene solution for 1 minute for deparaffinization. Thereafter, the specimen was dehydrated in graded alcohols. Finally, the specimen was stained using hematoxylin and eosin (H&E) staining system for histopathology, or was further used in study of CD117-immunohistochemistry without H&E staining (see 3.4).

3.5 CD117-immunohistochemistry

Each specimen was pretreated by microwaving the slide in citrate buffer solution at pH 6.4 for 5 minutes and slowly cooled down to retrieve CD117-antigens. Further, endogenous peroxidase activities in the specimen were eradicated by incubating the specimen with 3% hydrogen-peroxide at room temperature for 30 minutes, and washing after the incubation with sterile

phosphate buffer solution (PBS). Afterward, the specimen had been incubated by 1% bovine serum albumin (BSA) to block non-specific protein backgrounds at 37°C overnight and was washed in PBS. Thereafter, the specimen had been incubated by the polyclonal rabbit anti-human CD117 antibodies (Dako, Denmark) at the concentration of 1:100 at 37°C for 30 minutes, and was washed with PBS after the incubation. The antibodies were trapped by incubating the antibody-coated specimen with Envision™ peroxidase system (Dako, Denmark) for 30 minutes at room temperature and washed again with PBS after incubation. The specimen had been colorized by reacting with a chromogenic agent, 0.05% 3, 3' diaminobenzidine tetrahydrochloride in 0.01M Tris HCl at pH 7.6 combined with 0.03% H_2O_2 (DAB), for 5 minutes and washing with PBS to terminate the reaction. Soon after, the specimen was counterstained by Meyer's hematoxylin for 1 minute. Next, the specimen was washed in running tap water for 5 minutes to clean excessive stains. The specimen was immediately rehydrated in graded alcohols (70%, 80%, 90% and 100%, respectively). Ultimately, the non-specific backgrounds and artifacts were eliminated by soaking the specimen in xylene for 1 minute. The specimen was visualized using light microscopy (Webster et al. 2004 and Gil da Costa et al., 2007).

3.6 Specimen collection for CD117-immunocytochemistry, PCR, Flow Cytometric quantitative analysis and Flow cytometric cell sorting

Concurrently to the biopsy, three sets of fine-needle aspirated MCT (FNA-MCT) cells were individually collected from the tumor mass in each case using a sterile 21, 22, 23 and 24G1 needle and sterile disposable 3 ml syringe. The tumor was aspirated in unidirection. The first FNA-MCT cell collection was directly smeared on a clean silane-coated glass slide for use in CD117-immunocytochemitry study. The second was resuspended in 200 μl PBS until used for PCR meanwhile the latter was kept in 200 μl RPMI-1640 (Invitrogen, USA) for employing in the Flow cytometric quantitative analysis and flow cytometric cell sorting. Fifteen FNA-MCT cell suspensions were used for FCM-quantitative analysis because in a half of specimens could not be harvested FNA-MCT cells properly due to the masses were small. Ultimately, only oone specimen was used for FCM-cell sorting because of the limited number of FNA-MCT cells in suspensions.

3.7 CD117-immunocytochemistry

CD117-immunocytochemistry was run on the modified protocol previously used for study Melan-A immunocytochemistry in canine melanoma (Hoinghaus et al., 2002). Fresh FNA-MCT cells from the first collection in each case were smeared on a Silane-coated glass slide. The neoplastic cells were fixed in 4°C cold acetone for 5 minutes to preserve their morphologies and cellular proteins. As in CD117-immunohistochemistry, the endogenous peroxidase activities in the tumor cells were terminated by incubating the cells with 0.5% hydrogen peroxide (H_2O_2) in methanol at room temperature for 20 minutes and rinsing with Tris HCl at pH 7.5 for 10 minutes. Further, the non-specific backgrounds were blocked by 1% BSA (Sigma Aldrich, USA) at 37°C for 5 minute, washing the cells with PBS after incubation. Afterward, the cells was incubated with the polyclonal rabbit anti-human CD117 antibodies diluted by PBS in 0.5% BSA at the concentration of 1: 300 at 37°C for 30 minutes, washing the tumor cells with PBS for 5 minutes after incubation. Thereafter, the tumor cells had been incubated with Envision™ peroxidase System (Dako, Denmark) for 30 minutes and were washed in PBS for 5 minutes. Next, the tumor cells were colored by reacting with DAB chromogenic substrate (0.05% 3, 3' diaminobenzidine tetrahydrochloride in 0.01M Tris HCl at pH 7.5 combined with 0.03% H_2O_2) for 15 minutes, and washing with PBS to halt the reaction. Ultimately, the specimen had been counterstained by Meyer's hematoxylin solution for 5 minutes and was visualized under a light microscope.

3.8 Flow Cytometric Enumeration of FNA-MCT cells in a cell suspension

3.8.1 CD117-immunocytofluorescense

To identify the specificity of the PE-conjugated mouse monoclonal anti-human CD117 antibodies (Clone Y.B5.B8, Becton and Dickinson, US) to KITs and the affinity of KITs to antibodies, CD117-immunocytofluorescence was operated to define these two parameters. The protocol was slightly modified from CD117-immunocytochemistry protocol. Stepwise, the tumor cells were smeared on a silane-coated glass slide and fixed with 4°C cold acetone for 5 minutes to preserve their morphologies and proteins, drying the slide after preservation. 1% bovine serum albumin was added on the tumor cells for non-specific protein blockages for 30 minutes at room

temperature and then washing the slide. The tumor cells were further incubated with the PE-conjugated mouse monoclonal anti-human CD117 antibodies for 30 minutes at the concentration of 1:100 at room temperature in a dark chamber. After washing with PBS, the cells were counterstained by 4', 6-Diamidino-2-Phenylindole (DAPI, Invitrogen, USA) for nuclear staining. The stained tumor cells were visualized under a fluorescent microscope providing the 575 nm light source as shown in Figure 3.2.

Figure 3.2 The feature of fluorescence microscope used for CD117-immunocytofluorescence

3.8.2 Flow cytometric enumeration of total nucleated cells in a cell suspension

The estimated total number of nucleated cells in a cell suspension was enumerated using Flow cytometry method. The FNA-MCT cell suspension from the last collection was filtrated using a filter-capped BD Falcon™ collecting tube (Becton and Dickinson, USA). Other larger cells such as fibroblasts, fibrocytes, multinucleated giant cells if any, or large protein elements such as collagen and fibrous tissues in the suspension were separated from nucleated cells in this step. Of 10 μl sifted FNA-MCT cell suspension was pipetted and transferred into a BD Falcon™ collecting tube (Becton and Dickinson, USA). The aliquot of nucleated cell suspension was diluted and resuspended by 40 μl sterile PBS solution. Erythrocytes were lysed by 2 ml of BD Facs™-lysing solution for 10 minutes (Becton and Dickinson, USA), centrifuging at 1,400 rpm at room temperature for 5 minutes after RBC lysing and decanting the supernatant. Thereafter, the cell dreg of nucleated cells was resuspended by 300 μl sterile PBS. Ultimately, the data acquisition of total number of nucleated cells was accessed using BD FACScalibur™ flowcytometer with BD CellQuest™ software system (Becton and Dickinson, USA) as shown in Figure 3.3. The total number of nucleated cell in suspension was presented in unit of cells/ μl.

Figure 3.3 The feature of BD FACalibur™ flow cytometer used for Flow cytometric quantitative analysis in this study (from Becton and Dickinson, USA).

3.8.3 Flow Cytometric Enumeration of CD117-immunopositive cells in a cell suspension

Stepwise, to determine the total number of KIT-immunopositive cells in the suspension, Of 10 μl cell suspension formerly used in step 3.6.2 had been aliquoted into a BD Trucount™ tube (Becton and Dickinson, USA) before the cell suspension was diluted with 40 μl sterile PBS. Erythrocytes in the dilution were lysed using 2 ml of 1x BD Facs™-lysing solution (Becton and Dickinson, US) for 10 minutes, spinning down the cells at 1,400 rpm for 5 minutes at room temperature and discarding the supernatant. Afterward, the cells in sediment were pierced on their cell membranes by incubating them with 500 μl of 1x BD FacsPerm™ solution (Becton and Dickinson, US) for 10 minutes. Thereupon, the cells were washed by 2 ml sterile PBS for 10 minutes, centrifuging at 2,000 rpm for 5 minutes after washing, and decanting the supernatant. Forwardly, the cell sediment was incubated with the PE directly-conjugated mouse monoclonal anti-human CD117 antibodies (Clone Y.B5.B8, Becton and Dickinson, US) at concentration of 1:200 for 20 minutes in a dark chamber. Afterward, the cell dreg had been again washed with 2 ml of sterile PBS for 10 minutes and was centrifuged at 2,000 rpm for 5 minutes at room temperature, discarding the supernatant after centrifugation. The cell sediment was resuspended in 300 μl of sterile PBS. Ultimately, data acquisition was performed using FACScalibur™ Flow Cytometer with BD CellQuest™ software system (Becton and Dickinson, USA). The data was acquired as a percentage of KIT-immunopositive cells in the suspension. The final number of KIT-immunopositive cells in a cell suspension was finalized by converse the result from step 3.6.3. back to cells/μl by multiplying the data acquisited from 3.6.2 with the percentage of KIT-immunopositive cells collected from step 3.6.3. Therefore, the total amount of FNA-MCT cells in suspension was exhibited in unit of cells/ μl.

3.9 Flow Cytometric cell sorting

A 100 μl aliquot of cell suspension used in 3.6.2 was diluted and resuspended by 40 μl sterile PBS solution. After that, erythrocytes were eradicated by with 2 ml of BD Facs™-lysing solution for 10 minutes (Becton and Dickinson, USA), centrifuging at 1,400 rpm after lysing and discarding the supernatant. Soon after, the cell sediment was added by 500 μl BD FacsPerm™ solution (Becton and Dickinson, USA) for 10 minutes to increase membrane permeability. The cells were then washed using 2 ml sterile PBS solution for 10 minutes, spinning the cells down at 2,000 rpm for 5 minutes and discarding the supernatant. Thereafter, the cells were incubated in the dark chamber by the 100 μl of the PE directly-conjugated mouse monoclonal anti-human CD117 antibodies (Clone Y.B5.B8, Becton and Dickinson, USA) at concentration of 1:200 for 20 minutes. Afterward, the incubated cells had been again washed with 2 ml of sterile PBS and was centrifuged at 2,000rpm for 5 minutes at 25°C, decanting the supernatant after centrifugation. The cell dreg was resuspended in 2ml of sterile PBS. Ultimately, data acquisition was performed using BD-FACScalibur™ cell sorter with BD Cell-Sorting software system (Becton and Dickinson, USA). The sorted tumor cells were collected and kept in the collecting tube at -20°C until used for PCR.

3.10 DNA isolation from FNA- and FCM-sorted MCT cells

DNA from each specimen was extracted and purified by the commercial DNA isolation kit with the standard procedure recommended by the manufacture (Mobio, USA). 200 μl FNA-MCT cell suspensions in PBS were centrifuged at 10,000 x G for 1 minute, discarding supernatant after centrifugation. Afterward, the FNA-MCT cell dreg was homogenized by 700 μl of TD-1 solution included in the kit. The FNA-MCT cell sediment was vortex until the cells disappeared. The homogenized tumor cells in TD-1 solution was transferred onto a silica membrane-bounded collecting tube provided with the kit before centrifuging at 10,000 x G for 1 minute, discarding the supernatant after centrifugation. In this step, DNA was trapped on the filter. Forwardly, DNA-bounded on the filter was added with 400 μl of TD-2 solution from the kit, and was centrifuged twice at 10,000 x G for 1 minute to eradicate TD-2 solution. Unwanted contaminants were removed from DNA in this step. Ultimately, the silica-bounded DNA was eluted by 50 μl of the eluting solution TD-3, and was centrifuged at 10,000 x G for 1 minute to collect purified DNA in TD-3 solution in the collecting tube.

Then, the concentration of DNA extract in solution was measured by spectrophotometry (Appendix C). Ultimately, the DNA was kept at -20°C until used.

3.11 PCR analysis for exon-11 mutation in *c-kit* from FNA- and FCM-sorted MCT cells

3.11.1 dNTP preparation

In this study, the dNTP was prepared manually under the standard protocol as recommended by the manufacturer (Fermantas, USA). The initial concentration of each dNTP provided in the kit was 100 mM. 10 μl of each dNTP had been pipetted and was diluted by 460 μl Nuclease-Free Water. The final concentration of working dNTP solution was 2mM of each dNTP.

3.11.2 Primers

Both forward and reverse primers were designed from College of Veterinary Medicine, Michigan State University, USA. The forward and reverse primers were flanked from 5' end of exon-11 and 3' end of intron-11 in *c-kit*, respectively (Jones et al., 2004; Zavodovskaya et al., 2004). These primers were previously affirmed the specificity to exon-11 in *c-kit* in normal mast cells and MCT cells. The sequence for each primer was;

Forward primer; 5'-CCA TGT ATG AAG TAC AGT GGA AG-3'

Reverse primer; 5'-GTT CCC TAA AGT CAT TGT TAC ACG-3'

Both primers were synthesized and purchased from Biodesign™, Thailand. The initial concentration of each primer was 100 mM. The final concentration of each working primer was 10 mM prepared by diluting 10 μl of each stock primer with 90 μl of NFW. The DNA sequence of exon-11 in *c-kit* employed for primers setup is shown in Appendix B.

3.11.3 PCR positive, negative and normal controls

The positive control used for PCR was provided from College of Veterinary Medicine, Michigan State University, US. The genomic DNA (gDNA) in positive control was isolated and purified from the biopsy specimen obtained from one Golden Retriever MCT dogs which confirmed containing exon-11 mutation. The initial concentration of gDNA in positive control was

45.3 μg/ μl. The gDNA of normal control was extracted from the blood collected from one cross-bred dog in our laboratory. This dog was ratified to be free from MCT by the physical examination conducted by the author. The blood from this dog was also investigated to rule out mastocytosis and the result also confirmed a mastocytosis-free period in this dog. Finally, Nuclease Free Water was used as the negative control in this study.

3.11.4 PCR protocol

A 25 μl of PCR cocktail was manually prepared in a flat-capped PCR tube (Axygen, USA). The composition of PCR mixer consisted of the followings ingredients; 1.5 μl of 10X KCl buffer solution (DreamTaq™, Fermantas, USA), 1.5 μl of 10X $(NH_4)_2SO_4$ buffer solution (DreamTaq™, Fermantas, USA), 3 μl of 20mM $MgCl_2$ solution (Fermantas, USA), 1 μl of 2mM dNTP solution (Fermantas, USA), 0.5 μl of Taq polymerases (DreamTaq™, Fermentas, USA), 2 μl of 10mM Forward primers solution, 2 μl of 10mM Reverse primers solution, 4 μl of Purified DNA template and 9.5 μl of nuclease free water (NFW) (Promega, USA; Mobio, USA). Finally, the DNA template in the PCR mixer was amplified in the thermocycler (G-Storm™, USA) with the batch of programmatic temperatures for the thermocycler as; 95°C for 5 minutes for initial DNA denaturation; 40 cycles of 95°C 1 minute for cyclic DNA denaturation, 57-59°C for 1 minute for cyclic DNA Annealing and 72°C for 1 minute for cyclic DNA extension; and 72°C for 5 minute for complete DNA elongation. Ultimately, the PCR product was kept at -20°C until analyzed (Webster et al., 2006). The protocol for annealing temperature calculation is demonstrated in Appendix D.

3.12 Amplicon analysis

The EtBr-mixed agarose gel solution was casted in a PCR mould with an 8-wells comb (Appendix E). The gel was left to be cool down until it returned to the semi-solid state. The agarose gel had been placed in an electrophoresis buffer tray (Bio-Rad, USA) and was soaked by TAE solution. 5 μl of working 50-bp DNA ladders (GeneRuler™, Fermantas, USA) was used as the reference DNA marker in the first well. Further, 10 μl of each PCR product was separately pipetted and completely mixed with 8 μl of ready-mixed loading dye (Fermantas, USA). Each PCR product

was successively loaded into a well on agarose gel. Finally, the electrophoresis was run using 100V 100 V of direct current (DC) for 40 minutes.

The amplicons were visualized by the gel documentation machine (Bio-Rad, USA). The information was analyzed by the computerized software system, Quantity One™ version 4.6.9, (Bio-Rad, USA) with the standard instruction recommended by the manufacturer. The analyzed information was transformed and was kept in JPEG-imaging system using Microsoft paint (Microsoft, USA).

3.13 Interpretative criteria

3.13.1 Histopathologic interpretation

The interpretation for histopathologic diagnosis and grading for MCT was described using Patnaik histopathologic grading system. The tissue sections were evaluated by 3 veterinary pathologists. Two-third agreements from the pathologists were used to justify histopathologic grade. The interpretative criterions were established based on the tumor cell morphologies and their distributions in lesions as explained followings;

MCT-Grade I: Lesions in neoplasms are confined to the dermis and interfollicular spaces. Well-differentiated mast cells are arranged in rows or small groups of sheet pattern, separated by mature collagen fibers of the dermis. Tumor cells are round and monomorphic with ample cytoplasm. The tumor cells have distinct cytoplasmic boundaries and medium-sized, intracytoplasmic granules. Nuclei are round with condensed chromatin. Mitotic cells are absent (Patnaik et al., 1984).

MCT-Grade II: Neoplastic cells usually infiltrated or replaced the lower dermal and subcutaneous tissues. Some tumors extend to the skeletal muscles or surrounding tissues. The moderately pleomorphic cells are arranged in groups with thin to thick fibrovascular stroma. Fibrocollagenous fibres with hyalinization are commonly seen. The neoplastic cells are round to ovoid. Scattered spindle and giant cells are also observed. Most tumor cells have distinct cytoplasm with fine, intracytoplasmic granules. In some circumstances, the cytoplasm is indistinct and the granules are hyperchromatic. Nuclei are round to indent with scattered chromatin. Single nucleoli are

almost seen in lesions. Occasionally, some tumor cells have binuclei. Mitotic figures are rare might be ranging from 0 to 2 per high power field (Patnaik et al., 1984)

MCT-grade III: These neoplasms are cellular and pleomorphic, and neoplastic tissue replace subcutaneous and deeper tissues. The pleomorphic, medium-sized, round, ovoid, or spindleshaped neoplastic cells are arranged in closely packed sheets. The cytoplasm is indistinct with fine-intracytoplasmic granules or obscure granules. The stroma is fibrovascular or thick and fibrocollagenous with areas of hyalinization. The indented round to vesiculated nuclei have one or more prominent nucleoli. Binucleated cells are commonly observed. There are many giant cells and scattered multinucleated cells. Mitotic cells are also common, ranging from 3 to 6 cells per HPF (Patnaik et al., 1984).

3.13.2 CD117-immunohistochemistry and CD117-immunocytochemistry interpretations

The interpretative criterions for CD117-immunohistochemistry and -immunocytochemistry were dependant on CD117-immunoreactivity staining patterns. There were three staining patterns previously described in CD117-immunohistochemitry (Kiupel et al., 2004; Gil da Costa et al., 2007) and CD117-immunocytochemistry (Theerawatanasirikul et al., 2009) as; perimembrane, paranuclear and cytoplasmic-diffuse. The description of each staining pattern was explained as following;

Staining pattern I: CD117-immunoreactivity is predominantly presented on a cytoplasmic membrane. This pattern is usually referred as perimembrane pattern.

Staining pattern II: the immunopositivity is strongly stippled in cytoplasm close to a cytoplasmic surface of nuclear membrane. The synonym of this pattern is paranuclear or Golgi-like pattern.

Staining pattern III: the stains are vastly distributed throughout cytoplasm of tumor cells. This pattern is commonly named as Cytoplasmic-diffuse pattern in some literatures (Morini et al., 2004).

The interpretation was performed by 3 veterinary pathologists. The staining patterns were inspected in five highly-cellular areas. Two-third agreements in staining patterns were accepted and applied for determining the CD117-immunostaining patterns in respect specimens.

3.13.3 PCR analysis for exon-11 mutation in *c-kit* interpretation

The amplicon was visualized by the agarose gel electrophoresis and interpreted using these criterions;

Positive control or Mutant exon-11 containing MCT cells: the PCR product comprises of two or three distinguished bands (Figure 3.4 and 3.5, respectively); 191-bp, 250-bp and 280-bp. The 191-bp amplicon is the heterozygous normal allele and the 250-bp is the mutant exon-11 allele. The last band if any is the heterodimerization of normal and mutant alleles. This heteroduplex in general obstructs the movement of amplicon on agarose gel therefore it is usually presented as the most upper band on agarose gel (London et al., 1999; Jones et al., 2004; Zavodovskaya et al., 2004; Webster et al., 2006).

Normal control: the amplicon usually consists of the 191-bp homozygous normal allele presented on the agarose gel as the single band (Webster et al., 2006).

Negative control: there is usually no band presenting in agarose gel electrophoresis otherwise an artifact or a contaminant (Webster et al., 2006).

Figure 3.4 This figure depicts the double bands of normal allele and mutant exon-11 in *c-kit* allele. The ITD-mutant exon-11 amplicons are demonstrated at the upper bands (arrows) meanwhile the 191-bp amplicons at the base-line are normal alleles (Jones et al., 2004).

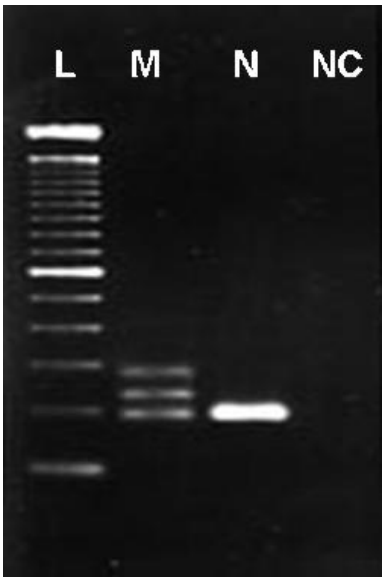

Figure 3.5 The PCR products of positive, normal and negative controls, the PCR product of this study consisted of the triple bands which different from the result in figure 3.4. The triple bands presented 191-bp normal allele, 250-bp mutant allele of exon-11 and 280-bp heteroduplex. The normal control exhibited the single band of 191-bp normal allele of amplicon (Webster et al., 2006).

CHAPTER IV

RESULTS

4.1 Clinically biological parameters

The age of MCT dogs in this study ranked from 7 to 15 years. There was no gender predilection seen in this study, male 56.67% (17/30) and female 43.33% (13/30), respectively. The most prevalent breed was cross-breed (16/30), Golden Retriever (5/30), Pug (2/30), respectively. The predilection sites of tumors were at the trunks, axilla, neck, inguinal and tail. The overview of clinically biological parameters was exhibited in Appendix A.

4.2 MCT histopathologic grading

Based upon, Patnaik histopathological grading system for MCT, the H&E sections of MCT-grade I displayed a uniformity of MCT cells in the sections. The lesions of tumors were confined in dermis layers of skins surrounded by very thin fibrovascular capsules. The tumor cells were well-differentiated arranging in sheet-like pattern. The tumor cells were uniquely round to oval in shape and approximately 10-15 μm in diameter. The cytoplasmic membrane boundaries were distinct. The cytoplasm was ample and eosinophillic. Metachromatic granules and refactile vacuoles were seen in cytoplasm of the neoplastic cells. Nuclei of tumor cells were round to oval with aggregated chromatin. The mitotic figures were rarely seen (Figure 4.1A).

In grade II, the neoplastic cells highly infiltrated into the lower dermis and underneath subcutaneous tissues. The tumor cells were moderately pleomorphic varying from round, oval to pyramidal in shape with 10-15 μm in size. They arranged in small groups with sheet-like in pattern supported by thick fibrovascular connective tissues. The spindle and giant tumor cells were also observed in some cases. Almost neoplastic cells were moderately-differentiated. The cytoplasm of almost tumor cells were distinct containing fine metachromatic granules stained in deep blue to purple by H&E. Nuclei were round to indent and hyperchromatic. Bi-nuclei tumor cells were found in some sections. The mitotic index was rarely seen, less than 2 per HPF (Figure 4.1B).

In grade III, the tumor cells were not confined in the dermis but vastly invaded to the surrounding tissues including underneath skeletal muscles. The boundary of neoplasms was indistinct. The morphology of neoplastics cells was atypical. These anaplastic cells shaped in round, oval, spindle, pyramidal or satellite with approximately 12-35 μm in size. The pleomorphism reflected in the less well-differentiation of tumor cells. The cytoplasm was indistinct with or without fine metachromatic cytoplasmic granules. The vacuolated cytoplasmic granules were readily seen in the cells. Thick fibrovascular were seen intervening throughout lesions. Almost neoplastic cells prominently contained indent vesiculated nuclei with one or more nucleoli. Binucleated cells were commonly observed in lesions. There were many giant cells or multinucleated cells seen in some circumstances. The mitotic cells were also common ranging from 3 to more than 5 cells per high power field (Figure 4.1C).

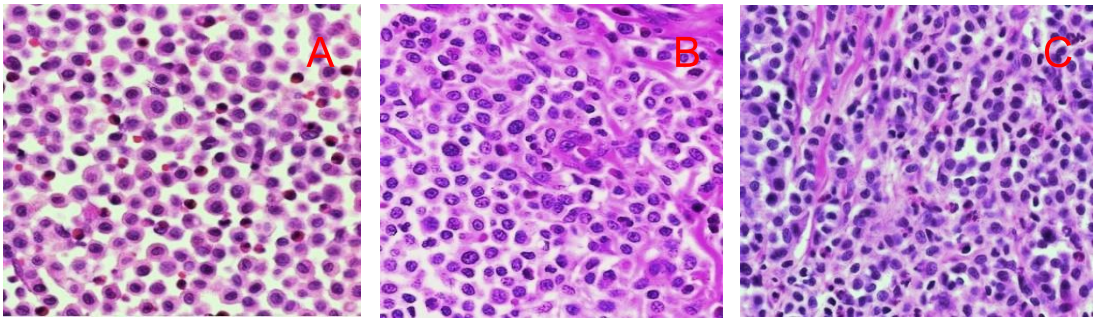

Figure 4.1 The figure illustrates the histopathologic appearance of MCT in each grade; grade I (A), grade II (B) and grade III (C), based upon Patnaik histopathologic grading system.

In this study, of thirty MCT specimens were classified into 3 groups depending on their respective grades. 12 out of 30 MCT specimens were classified for MCT-grade I, 11 for grade II and 7 for grade III, respectively. The distribution of three histopathological grades in thirty MCT specimens is recapitulated in Table 4.1.

Table 4.1 The total number of specimens in each histopathological grade classified on Patnaik histopathological grading system

	MCT-grade I	MCT-grade II	MCT-grade III	Total
Specimen No.	12	11	7	
				30 Specimens

4.3 CD117-immunohistochemistry

Three CD117-Immunohistochemisty staining patterns were identified in this study; perimembrane (pattern I), paranuclear (pattern II) and cytoplasmic diffuse patterns (pattern III). All three CD117-immunohistochemical staining patterns are depicted in Figure 4.2.

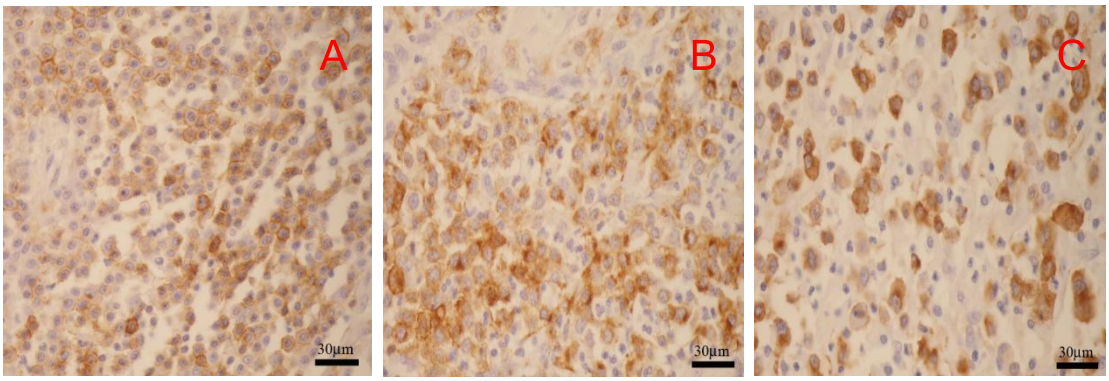

Figure 4.2 Three CD117-immunohistochemistry staining patterns found in this study are shown in this picture (400X); perimembrane (A), para-nuclear (B) and Cytoplasmic diffuse (C)

4.4 CD117-immunocytochemistry

The CD117-immunolabeling patterns in FNA-MCT cells were compatible to those previously described in CD117-immunohistochemistry. Three staining patterns of CD117-immunocytochemistry were identified in this study. The first was perimembrane (pattern I). The second was paranuclear (pattern II) and the last one was cytoplasmic diffuse (pattern III) as found in CD117-immunohistochemistry (Figure 4.3).

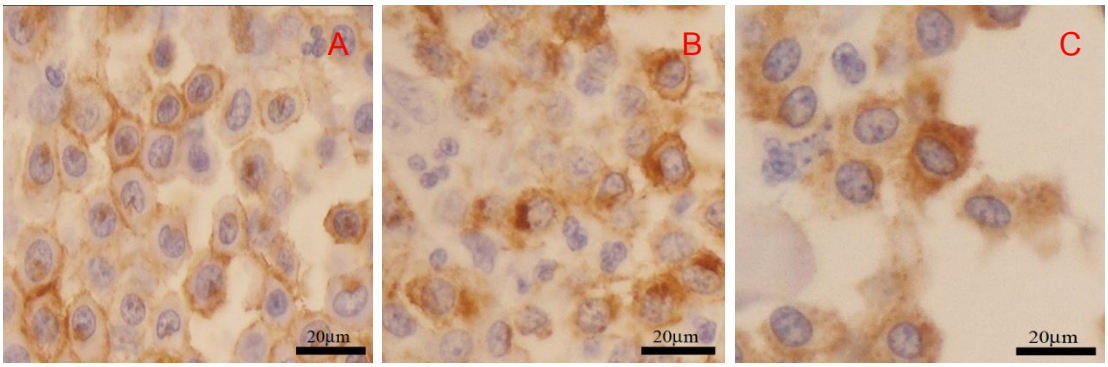

Figure 4.3 This picture depicts three distinct CD117-immunocytochemistry staining patterns; perimembrane (A), paranuclear (B) and cytoplasmic diffuse (C), which mimic to the staining patterns seen in CD117-immunohistochemistry.

The correlations of CD117-immunocytochemitry staining patterns to histopathological grades and CD117-immunohistochemistry staining patterns is presented in Table 4.2 and Appendix A.

Table 4.2 The relevance of CD117-immunocytochemistry staining patterns to histopathological grades and CD117-immunohistochemistry staining patterns

30 MCT Specimens					
MCT-grade I 12/30		MCT-grade II 11/30		MCT-grade III 7/30	
CD117-IHC	CD117-ICC	CD117-IHC	CD117-ICC	CD117-IHC	CD117-ICC
Pattern I n = 8	n = 8	n = 2	n = 2	n = 1	n = 2
Pattern II n = 3	n = 3	n = 6	n = 6	n = 4	n = 4
Pattern III n = 1	n = 1	n = 3	n = 3	n = 2	n = 1
100 % Compatible		100 % Compatible		85.72% Compatible	

4.5 Flow cytometric quantitative analysis

Before all flow cytometric subprocedures were performed, CD117-immunocytofluorescence had been processed for evaluating the specificity and affinity between the antibodies and KIT to ensure that the sorted cells were MCT cells. CD117-immnocytofluoresence suggested that the antibodies were suitable to be applied in cell sorting. Almost cells were substantially positive to the antibodies. Under the fluorescence microscope, the CD117-immunopositive MCT cells are stained red in their cytoplasm and on their cytoplasmic membranes. All nuclei were stained blue by DAPI as shown in Figure 4.4. There were some cells of which their cytoplasm did not be stained, presumably were non-MCT cells in the suspension.

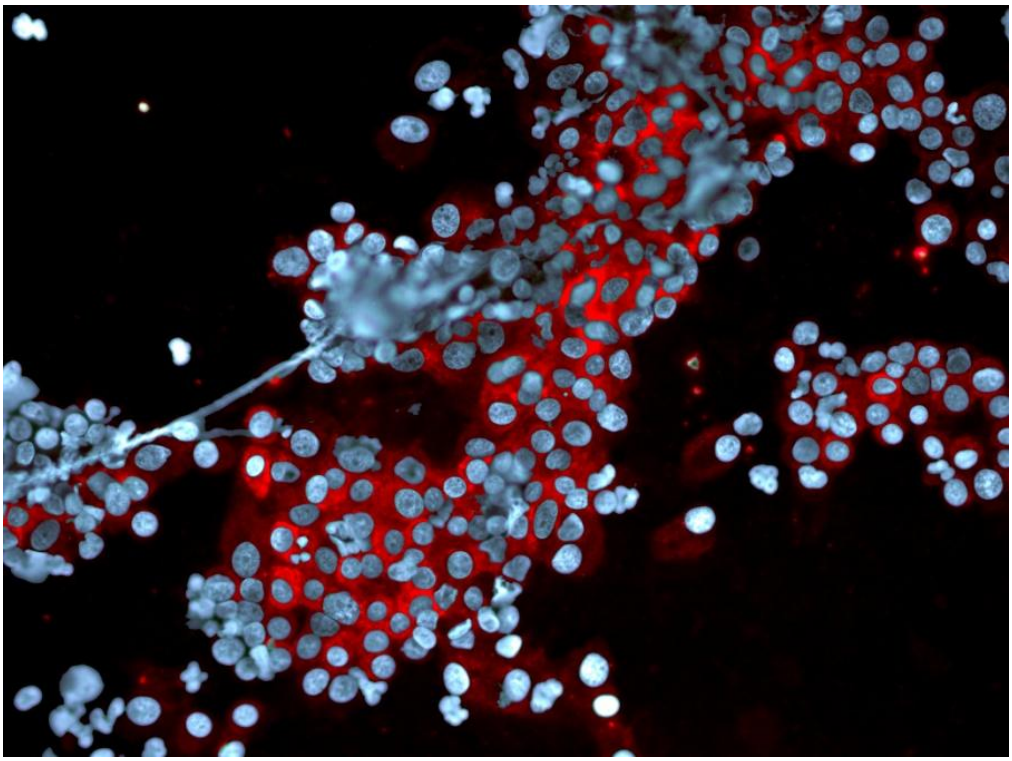

Figure 4.4 The result of CD117-immunocytofluorescence using PE-conjugated monoclonal anti-human antibodies depicted cytoplasmic CD117-immunostaining of FNA-MCT cells. The nuclei of all cells have been counterstained by DAPI. Note; there are some cells have been stained only in nuclei by DAPI without cytoplasmic staining. This suggests that in the cell suspension consisting of two sub-populations inside; MCT and non-MCT cells

The enumeration of FNA-MCT cells was performed using Flow Cytometry. As previously described, the total number of nucleated cells in the suspension was acquisitioned in the unit of cells/μl. The second step provided the net percentage of CD117-immunopositive cells in the same suspension; of which were the FNA-MCT cells. The final result was then calculated back by multiplying the total number of nucleated cells in the suspension with the net percentage of CD117-immunopositive cells in cells/μl. In this study, 15 out of 30 chosen MCT specimens were picked out and employed for flow cytometric quantitative analysis. The remaining specimens were not performed flow cytometric quantitative analysis because of the limitation in specimen collections. The average total number of nucleated cells was 17,417 cells/μl; meanwhile the average of net percentage of CD117-immunopositive cells was 40.69% and the average total number of FNA-MCT cells was 6,345 cells/μl (6,345,000 cells/ml); of which enough for PCR analysis of exon-11 mutation in *c-kit*. The big picture of all fifteen FNA-MCT cell specimens in flow cytometric quantitative analysis is summarized in Table 4.3

Table 4.3 The Flow cytometric enumerations of FNA-MCT immunopositive cells in 15 FNA-MCT cell suspensions. The average number of FNA-MCT cells in suspension is 6,345 cells/μl, Note; BDTrucount™ bead number is varied depending upon the manufacture determinations

Specimen No.	1	2	3	4	5	6	7	8
Amount of nucleated cells in suspension (cells/μl)	21,025	21,008	3,773	45,680	3,727	38,442	3,771	46,351
BDTrucount™ Bead No.	50,441	50,441	50,979	49,219	50,979	49,133	50,979	50,441
Percent of CD117-Immunopositive Cells	14.99%	87.32%	17.78%	87.31%	22.25%	15.3%	18.71%	40.25%
Amount of CD117-Immunopositive cells in suspension (cells/μl)	3,152	18,344	671	4,959	829	5,882	697	18,656

Specimen No.	9	10	11	12	13	14	15	
Amount of nucleated cells in suspension (cells/μl)	12,164	5,538	14,232	4,413	3,812	22,332	14,985	
BDTrucount™ Bead No.	50,441	49,219	50,979	50,441	50,979	50,441	49,219	
Percent of CD117-Immunopositive Cells	94.91%	40.26%	14.84%	8.84%	21.84%	82.21%	43.59%	
Amount of CD117-Immunopositive cells in suspension (cells/μl)	11,545	2,230	2,112	390	833	18,339	6,532	
Average amount of FNA-MCT cells in suspension (cells/μl)								6,345cells/μl

4.6 PCR analysis of exon-11 mutation in *c-kit* from Fine-needle aspirated MCT cells

Measurements of DNA concentration from FNA-MCT cells of 30 selected MCT specimens had been performed before the analysis of exon-11 mutation in *c-kit* by PCR was processed. The average concentration of DNA was 120.45 μg/ml. The result of DNA concentration measurements in all specimens was recapitulated in Table 4.4.

Table 4.4 The table provides each λ_{260} value of DNA from individual respect FNA-MCT cell suspension measured by spectophotometry and its transformed concentration in μg/ml at dilution factor of 100.

Specimen No.	1	2	3	4	5	6	7	8	9	10	11	12	13	14	15
OD-ABS	0.110	0.110	0.148	0.111	0.120	0.098	0.104	0.091	0.155	0.231	0.218	0.251	0.385	0.288	0.313
DNA Concentration (μg/ml)	55	55	74	55.5	60	49	52	45.5	77.5	115.5	109	125.5	192.5	144	156.5
Specimen No.	16	17	18	19	20	21	22	23	24	25	26	27	28	29	30
OD-ABS	0.176	0.209	0.187	0.314	0.311	0.422	0.194	0.610	0.383	0.405	0.396	0.143	0.257	0.34	0.147
DNA-Concentration (μg/ml)	88	104.5	93.5	157	155.5	211	97	305	191.5	202.5	198	71.5	128.5	170	73.5
Average Concentration (μg/ml)															120.45

Upon PCR analysis, the result suggested that the standard PCR could be employed to study the exon-11 mutation in *c-kit* from FNA-MCT cells. The amplicons of positive control and mutant exon-11 containing specimen composed of two separated bands; 191-bp normal allele and 250-bp mutant allele. Meanwhile, the normal control and specimens containing non-mutant exon-11 consistently showed the single band of 191-bp normal alleles. The negative control exhibited no band in the every PCR analysis. There was only one specimen (3.33%) containing exon-11 mutation in *c-kit* observed in this study. According to Patniak histopathologic grading system, this specimen was classified as MCT-grade II. The positive result of PCR in this case is illustrated in Figure 4.5. It is noteworthy that the PCR product of this specimen had been shown 191-bp normal

allele in our preliminary study. The total number of mutation and non-mutant exon-11-containing FNA-MCT specimens is depicted in Table 4.5.

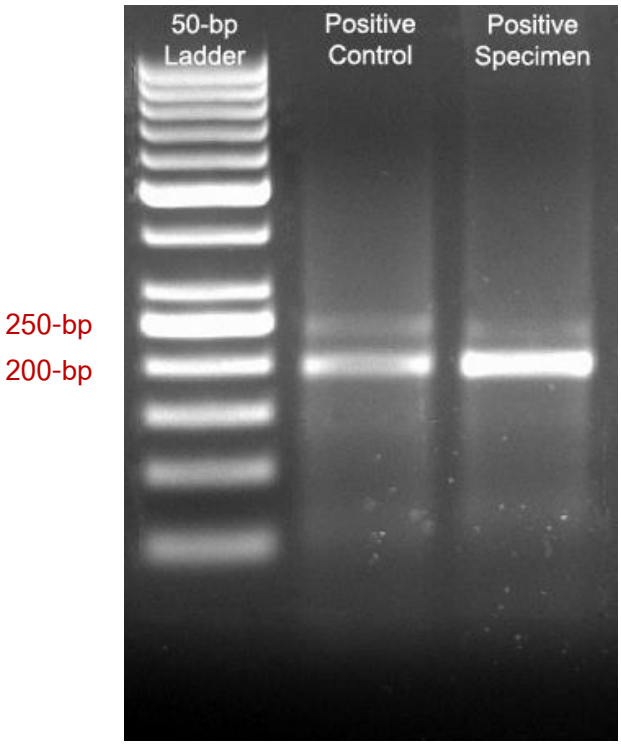

Figure 4.5 The figure shows the positive results of PCR using DreamTaq™ Polymerase. From the left to right, in the first lane is 50-bp DNA marker, the middle is the positive control and the last one represents the PCR positive result from the specimen.

Table 4.5 The summation of the total numbers of mutant- and non-mutant exon-11-contaiining FNA-MCT specimens in this study

	Number of studied specimens	Number of specimens	Percentage
Mutant exon-11	30	1	(3.33 %)
Non-mutant exon-11	30	29	(96.67 %)

In addition, the 191-bp DNA strip of each amplicon on agarose gel from the positive control, normal control and three specimens was isolated and collected for DNA sequencing. All DNA sequences were identical to one another. The result consistently represented 191-bp DNA sequence of exon-11 in *c-kit*. This result reinforced that DNA extracts were from MCT cells including the specificity of primers used in this study. The DNA sequences were depicted in Figure 4.6 below.

Figure 4.6 The DNA sequence analysis of normal allele of exon-11 in the positive control, negative control and three specimens. Note; the sequences are identical to one another.

4.7 PCR analysis of exon-11 mutation in *c-kit* from Flow cytometric-sorted MCT cells

One specimen from 15 specimens formerly used for Flow cytometric quantitative analysis was operated for Flow Cytometric cells sorting to separate MCT cells from other cells in the suspension. According to the specificity of the antibodies to KITS, therefore; the CD117-Immunopositive cells were sorted out from the suspension during the operation. In total of 400,000 FCM-sorted MCT cells were harvested from the FCM-cell sorting in this case. The cell suspension was hundred-fold and thousand-fold diluted by PBS. DNA of the tumor cells from both dilutions was extracted and purified using the same protocol used in 4.6 before proceeding PCR analysis for exon-11 mutation. The outcome of PCR demonstrated at the thousand-fold dilution, the targeted DNA could not be amplified by PCR, meanwhile at the hundred-fold dilution; the 191-bp amplicons were amplified using PCR. DNA was also isolated from the biopsied tissue in the same case to enhance

the stability of PCR analysis for exon-11 mutation in *c-kit*. The comparative results from all procedures were consistently similar to one another as exhibited in Figure 4.7.

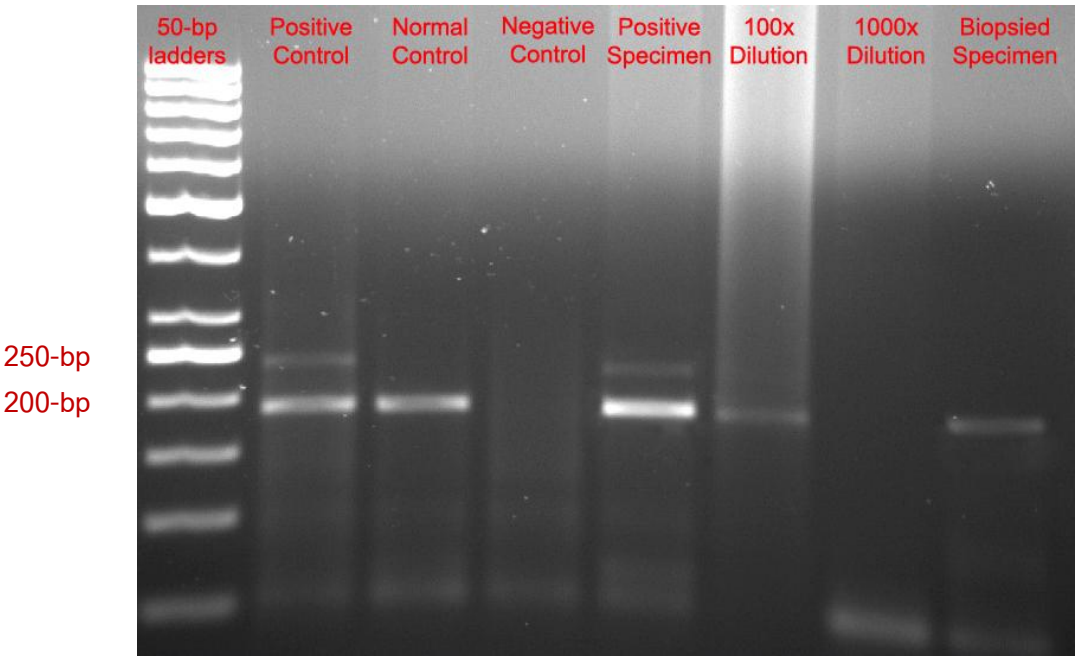

Figure 4.7 The PCR results of hundred-fold dilution and thousand-fold dilution of FCM-sorted MCT cells were shown in lane 6 and 7, respectively. In hundred-fold dilution the DNA was still amplified but in the thousand-fold dilution, the amplicon could not be amplified suggesting that the lowest concentration of MCT cells in the suspension should be at least 4,000 cells /μl. The last lane was the respresentative of 191-bp amplicon of which DNA extracted from the biopsy specimen.

CHAPTER V

DISCUSSION AND CONCLUSION

Discussion

In this study, the ages of MCT dogs were varied from 6 to 18 years with the average of 9.1 years. The most three prevalent ages of MCT dogs was 10 (23.33%, 7/30), 12 (13.33%, 4/30) and 7 (10%, 3/30) years, respectively. Many previous studies have demonstrated that there was no gender predilection associating in MCT incidence or survival time (Thamm and Vail, 2007; Welle et al., 2008). However, one European study demonstrated that female MCT dogs had a more favorable prognosis with chemotherapy than their male counterparts of which a difference in sex hormone profiles of both genders might be a causative factor affecting on tumor behavior (Thamm and Vail, 2007; Welle et al., 2008). The result on gender predilection in this study suggested that there was no gender predilection seen in the study. There were male (56.67%, 17/30) and female (43.33%, 13/30) MCT dogs participating in this study, respectively. Moreover, the most three prevalent breeds observed in this study were cross-breed (16/30), Golden Retriever (5/30) and Pug (2/30), respectively. In general, canine cutaneous MCT are commonly showing up on the trunks (50–60%), extremities (25-40%), and the head and neck (10%). The scrotum, perineum, back and tail are less commonly observed (Welle et al., 2008). The predilection sites of tumors found in this study were also correlated to those described previously. The most affected sites were on the ventro-lateral of the trunks especially axillary regions, the necks, the inguinal areas and the tails. In addition, hematologic bioparameters were not employed for data interpretation but were included in this study.

Basically, MCT diagnosis and prognosis is performed based on various histopathological parameters such as cellular differentiation, mitotic rate and tumor invasion. These parameters may be helpful for predicting a tumor biological behavior, grading and prognosis, in some circumstances (Welle et al. 2008). Nowadays, there are two histopathological grading schemes used for MCT diagnosis issued by Bostock and colleagues in 1973 and Patnaik et al. in

1984. In addition, the other parameters reportedly used for MCT diagnosis, grading and prognosis to date are clinical stage, tumor location, breed, growth rate/duration, PCNA, tumor recurrence, AgNOR count and intratumoral vessel density (Dank 2005).

In this study, three CD117-immunohistochemisty staining patterns were identified; perimembrane (pattern I), paranuclear (pattern II) and cytoplasmic diffuse patterns (pattern III). Almost MCT specimens had CD117-immunolabeling pattern II (43.33 %) followed by pattern I (36.67 %) and III (20%), respectively. The staining pattern I was distributed abundantly in MCT-grade I, like wise pattern II in grade II and pattern III in grade III, suggesting a tendency to find a higher staining pattern in higher MCT grade. Besides, the distribution of each staining pattern in this study was closed to those reported in previous studies (Kiupel et al., 2004; Morini et al., 2004; Webster et al., 2006; Gil da Costa et al., 2007). Furthermore, the aberrant cytoplasmic CD117-immunopositivity associated with *c-kit* mutation might indicate a poor prognosis in MCT, such as decreased survival time or increased risk of tumor relapse, owing to the aggressive biologic behavior always correlate with an increased cytoplasmic staining of KIT (Kiupel et al., 2004; Morini et al., 2004; Webster et al., 2006; Gil da Costa et al., 2007). In addition, the extra advantage of CD117-immunohistochemistry is the usage to clarify MCT from other round cell tumors.

From CD117-ICC assay of FNA-MCT cells, the consequence has exhibited that the CD117-ICC staining patterns were resemble to CD117-IHC staining patterns. The distribution of a CD117-ICC staining pattern in specimens when compared with CD117-IHC, case-by-case, was 85.72 % compatible. Because in one case; there was a nuance between CD117-ICC and CD117-IHC staining pattern. In this case, it contained staining pattern I when defined by CD117-ICC, meanwhile staining pattern III in CD117-IHC. This incompatibility might point out an error on the FNA direction that could not cover all regions of the tumor mass resulting in the miss of targeted neoplastic cells. In addition, the cell loss from preparatory process in this case might also affect to this point.

The enumeration of FNA-MCT cells in this study was performed using Flow cytometry. Before processing all FCM-subprocedures, CD117-Immunocytofluorescence was done. The consequence indicated the specificity of antibodies to KIT proteins and the affinity of FNA-MCT cells to the antibodies. Although, other cell types such as melanoma and some monocytoid B-cells

could be positively stained with the antibodies, but in this period, most FNA-cells had been confirmed that they were MCT cells by giemsa staining before performing CD117-immunocytofluorescence. Therefore, it was believably that all FNA-cells in this study were FNA-MCT cells. The result from this step has suggested that Flow cytometry can facilitate in the enumeration of FNA-MCT cells in a suspension with the average of 6,345 cells/ μl in a cell suspension. Moreover, the result has been emphasized that these FNA-MCT cells were the representative of whole FNA-MCT cells in a tumor mass which were obtainable by FNA.

In mammalian (human, dog, cat, cow, goat, rat, and mouse), juxtamembrane domain of KIT consists of 38 amino acid residues (residues 543-580) which identical in one another (Ma et al., 1999). This intracellular domain of KIT is encoded by exon-11 in *c-kit* proto-oncogene. Several studies have shown that a mutation of exon-11 in *c-kit* should participate in MCT tumorigenesis (London et al., 1999; Webster et al., 2006). The incidence of exon-11 mutation in *c-kit* has been reported varying from 9-30 % in MCT biopsied specimens (Downing et al., 2002; Zemke et al., 2002; Webster et al., 2006; Letard et al., 2008; Thompson et al., 2011) as well as in C1 and C2 cell lines (Ma et al., 1999; Downing et al., 2002). Nevertheless, exon-11 mutation in *c-Kit* might associate with a worse prognosis for MCT dogs (Zemke et al. 2002). A large study on MCT dogs from several investigators indicating that the most common mutation of exon-11 in *c-kit* is 44 to 70-bp ITD at 3' end of exon-11 (Zemkee et al., 2002; Webster et al., 2006; Letard et al., 2008). Protein molecular assays in that study suggested that a tandem repeat in juxtamembrane domain of KIT depended on a specific ITD, for examples Asp575-Arg589, Pro576-Asn590, and Pro576-Arg59. There was on duplication resulting in the insertion of Gly residue after Phe594 followed by a direct repeat of residues Pro576-Phe594 was observed in the study. The information from a previous study also demonstrated that a mutation might associate to a higher grade of tumor but not between breed and grade (Zemkee et al. 2002). According to multivariable analysis in one study, the result demonstrated that MCT dogs containing ITD mutation of exon-11 in *c-kit* had significantly decreased survival times, increased incidence of mortality and increased incidence of recurrence both at the original and distant sites (Kiupel et al., 2004).

The characteristic in PCR analysis of exon-11 mutation in *c-kit* in amplicons from biopsied specimens in many previous studies has demonstrated that the PCR products consisted of

two or three separated bands on agarose gel electrophoresis. The bands were 191-bp of normal allele, 250-bp of mutant allele and 280-bp of heteroduplex between normal and mutant alleles, if any. However, the difference in number of DNA bands in PCR products is not significantly. The incidence of exon-11 mutation in previous studies was 9-33% in all biopsied specimens whereas 30–50% of MCT-grade II and -grade III possess activating ITD mutations of exon-11 in c-*kit* (Jones et al., 2004; Webster et al., 2006).

The PCR result from this study has shown two separated bands in amplified positive control and one specimen. The positive amplicons comprised of 191-bp and 250-bp DNA bands mimic to those described in former studies. However, in our preliminary study, the result has demonstrated that three separated DNA bands in amplicons of the positive controls and specimens were observed. Moreover, 3 specimens in that study contained the ITD-mutations meanwhile in this study only one MCT-grade II specimen had the mutation. Interestingly, this one mutant specimen had been approved that it did not contain exon-11 mutation in our preliminary study.

Based on the PCR result, it has reinforced that FNA-MCT cells could be used as a source for identifying a mutation of exon-11 in *c-kit* as in biopsied specimens. However, the incidence of positive specimen was 3.33% which lower than in biopsied specimens. Moreover, the decreased mutant specimens in this study might point out the loss of targeted FNA-MCT cells due to the unidirection or misdirection in FNA protocol.

In the comparative PCR analysis of exon-11 mutation in *c-kit* from FNA-MCT cells obtained directly from a mass with FCM-sorted FNA-MCT cells. FCM-cell sorting was firstly performed in one specimen. In total of 400,000 sorted FNA-MCT cells were harvested from this step and kept in 1 ml PBS before analysis. The consequence has accentuated that Flow cytometry could be applied for separating and collecting FNA-MCT from other mixed cells in a suspension. By the next step, the cell suspension was hundred-fold and thousand-fold diluted by PBS and the genomic DNA of the tumor cells from both dilutions was extracted and purified before proceeding PCR analysis. The outcome of PCR demonstrated at the thousand-fold dilution (400 FNA-MCT cells), the targeted amplicon could not be amplified by PCR, meanwhile at the hundred-fold dilution (4,000 FNA-MCT cells); the 191-bp PCR product was amplified. The result suggested that in a suspension,

there should have been at least 4,000 FNA-MC cells in suspension which would be enough for OCR analysis. The genomic DNA was also isolated from the biopsied tissue and FNA-MCT cells directly harvested from the mass, in this case to assure the stability of PCR analysis for exon-11 mutation in *c-kit*. The comparative results from all procedures were consistently similar to one another.

Conclusion

In conclusion, CD117-ICC could be applied for diagnosing MCT because of its high compatibility of the distribution of 117-ICC staining patterns to CD117-IHC in the same specimens. Moreover, the PCR result from this study has substantially demonstrated that Fine-needle aspirated MCT cells can be used for study the mutation of exon-11 in proto-oncogene *c-kit* by PCR method. Moreover, the results also exhibited that per one aspiration, FNA could provide an enough amount of FNA-MCT cells approved by Flow cytometric quantitative analysis. These cells could be employed for DNA extraction and purification before operating PCR.

Suggestions for further studies

1. Histopathologic grading should be switched from Patniak histopathologic grading system to be 2-tier histopathologic grading system which classifying MCT into low- and high-grade. Because this system recently provides a more accuracy in MCT grading and prognosticating and reduces an ambiguous inter-observation in MCT grading especially in MCT-grade II (Kiupel et al., 2011).
2. A number of specimens should be increased to ensure that any protocol described in this study will provide the consistent results.
3. FNA must be performed in multidirection to assure that the protocol will collect targeted MCT cells.
4. PCR analysis must be doubly executed in a mass study to warrant that PCR analysis for exon-11 mutation in *c-kit* from FNA-MCT cells is reproducibly and consistently.

5. Prolong monitoring of clinical parameters especially survival times and recurrences must be done to find out the correlation between these parameters with the consequence from PCR analysis for exon-11 mutation in FNA-MCT cells.
6. The relationship between exon-11 mutation in *c-kit* assayed by PCR in FNA-MCT cells with aberrant KIT localization in FNA-MCT cells should be done as operated in previous studies in biopsied specimens (Webster et al., 2006; Webster et al., 2007).

REFERENCES

Abraham, S.N. and St. John, A.L. 2010. Mast cell-orchestrated immunity to pathogens. Nat. Rev. Immunol. 10: 441-452.

Austen, K.F. and Boyce, J.A. 2001.Mast cell lineage development and phenotypic regulation. Leukemia. Res. 25: 511–518.

Bostock, D.E. 1973. The prognosis following surgical removal of mastocytomas in dogs. J. Small. Anim. Pract. 14: 27-41.

Conti, P., Castellani, M.L., Kempuraj, D., Salini, V., Vecchiet, J., Tetè, S., Mastrangelo, F., Perrella, A., De Lutiis, M.A., Tagen, M. and Theoharides, T.C. 2007. Role of mast cells in tumor growth. Ann. Clin. Lab. Sci. 37 (4): 321-339.

Culmsee, K. and Nolte, L. 2002. Flow cytometry and its application in small animal oncology. Meth. Cell. Sci. 24: 49-54.

Dank, G. 2005. Canine Mast Cell tumors. Isr. J. Vet. Med. 60(2): 67-68.

Dobson, J.M. and Scase, T.J. 2007. Advances in the diagnosis and management of cutaneous mast cell tumours in dogs. J. Small. Anim. Pract. 48: 424-431.

Downing, S., Chien, M.B., Kass, P.H., Moore, P.E. and London, C.A. 2002. Prevalence and importance of internal tandem duplications in exon 11 and 12 of *c-kit* in mast cell tumors of dogs. Am. J. Vet. Res. 63 (12): 1718-1723.

Duncan, J.R. and Prasse, K.W. 1979. Cytology of canine cutaneous round cell tumors, mast cell tumor, histiocytoma, lymphosarcoma and transmissible venereal tumor. Vet. Pathol. 16: 673-679.

Edling, C.E. and Hallberg, B. *2007.* Molecule in focus: c-Kit, c-Kit-A hematopoietic cell essential receptor tyrosine kinase. Int. J. Biochem. Cell. Biol. 39: 1995-1998.

Escribano, L., Orfao, A., Díaz-Agustin, B., Villarrubia, J., Cerveró, C., López, A., Marcos, M.A., Bellas, C., Fernández-Cañadas, S., Cuevas, M., Sánchez, A., Velasco, J.L., Navarro, J.L. and Miguel, J.F. 1998. Indolent systemic mast cell disease in adults: immunophenotypic characterization of bone marror mast cells and its diagnostic implications. Blood. 91 (8): 2731-2736.

Eurell, J.A. and Van, Stickle D.C. 2006. Connective and supportive tissue. In: Dellmann's Textbook of Veterinary Histology. J.A., Eurell and B.L., Frappier. 6thed. Iowa: Blackwell. 34-35.

Gil da Costa, R.M., Matos, E., Rema, A., Lopes, C., Pires, M.A. and Gärtner, F. 2007. CD117 immunoexpression in canine mast cell tumours: correlations with pathological variables and proliferation markers. B.M.C. Vet. Res. 3 (19): 1-7.

Govier, S.M. 2003. Principles of treatment for mast cell tumors. Clinical Techniques in Small Animal Practice. 18(2): 103-106.

Hill, P.B. and Martin, R.J. 1998. A review of mast cell biology. Vet. Dermatol. 9: 145-166.

Hoinghaus, R., Mischke, R. and Hewicker-Trautwei, M. 2002. Use of immunocytochemical techniques in canine melanoma. J. Vet. Med. A. 49:198-202.

Hubbard, S.R. and Till, J.H. 2000. Protein tyrosine kinase structure and function. Annu. Rev. Biochem. 69: 373–398.

Jones, C.L.R., Grahn, R.A., Chien, M.B., Lyons, L.A. and London, C.A. 2004. Detection of c-kit mutations in canine mast cell tumors using fluorescent polyacrylamide gel electrophoresis. J. Vet. Diagn. Invest. 16: 95-100.

Kaesnikoff, J. and Galli, S.J. 2008. New developments in mast cell biology. Nat. Immunol. 9 (11): 1215-1223.

Kiupel, M., Webster, J.D., Kaneene, J.B., Miller, R. and Yuzbasiyan-Gurkan, V. 2004. The use of KIT and tryptase expression patterns as prognostic tools for canine cutaneous mast cell tumors. Vet. Pathol. 41: 371–377.

Kiupel, M., Webster, J.D., Bailey, K.L., Best, S., DeLay, J., Detrisac, C.J., Fitzgerald, S.D., Gamble, D., Ginn, P.E., Goldschmidt, M.H., Hendrick, M.J., Howerth, E.W., Janovitz, E.B., Langohr, I., Lenz, S.D., Lipscomb, T.P., Miller, M.A., Misdorp, W., Moroff, S., Mullaney, T.P., Neyens, I., O'Toole, D., Ramos-Vara, J., Scase, T.J., Schulman, F.Y., Sledge, D., Smedley, R.C., Smith, K., Snyder, P.W., Southorn, E., Stedman, N.L., Steficek, B.A., Stromberg, P.C., Valli, V.E., Weisbrode, S.E., Yager J., Heller, J. and Miller, R. 2011. Proposal of a 2-tier histologic grading system for canine cutaneous mast cell tumors to more accurately predict biological behavior. Vet. Pathol. 48(1): 147-155.

Leeson, C.R., Leeson, T.S. and Paparo, A.A. 1985. Connective tissue proper. In: Textbook of Histology. C.R., Leeson and T.S., Leeson. 5th ed. Philadephia: W.B. Saunders. 112-114.

Letard, S., Yang, Y., Hanssens, K., Palmerini, F., Leventhal, P.S., Guery, S., Moussy, A., Kinet J.P., Hermine, O. and Dubreuil, P. 2008. Gain-of-function mutations in the extracellular domain of KIT are common in canine mast cell tumors. Mol. Cancer. Res. 6(7): 1137-1145.

Li, C.Y. 2001. Diagnosis of mastocytosis-value of cytochemistry and immunohistochemistry. Leuk. Res. 25: 537–541.

London, C.A., Galli, S.J., Yuuki, T., Hu, Z.Q., Helfand, S.C., Geissler, E.N. 1999. Spontaneous canine mast cell tumors express tandem duplications in the proto-oncogene *c-kit*. Exp. Hematol. 27: 689–697.

London, C.A., Hannah, A.L., Zadovoskaya, R., Chien, M.B., Kollias-Baker, C., Rosenberg, M., Downing, S., Post, G., Boucher, J., Shenoy, N., Mendel, D.B., McMahon, G. and Cherrington, J.M. 2003. Phase I dose-escalating study of SU11654, a small molecule receptor tyrosine kinase inhibitor, in dogs with spontaneous malignancies. Clin. Cancer. Res. 9: 2755–2768.

London, C.A. and Seguin, B. 2003. Mast cell tumors in the dog. Vet. Clin. Small. Anim. 33: 473–489.

London, C.A. 2009. Tyrosine kinase inhibitors in veterinary medicine. Top. Companion. Anim. Med. 24 (3): 106-11.

London, C.A., Malpas, P.B., Wood-Follis, S.L., Boucher, J.F., Rusk, A.W., Rosenberg, M.P., Henry, C.J., Mitchener, K.L., Klein, M.K., Hintermeister, J.G., Bergman, P.J., Couto, G.C., Mauldin, G.N. and Michels, G.M. 2009. Multi-center, placebo-controlled, double-blind, randomized study of oral toceranib phosphate (SU11654), a receptor tyrosine kinase inhibitor, for the treatment of dogs with recurrent (either local or distant) mast cell tumor following surgical excision. Clin. Cancer. Res. 15 (11): 3856-3865.

Ma, Y., Longley, B.J., Wang, X., Blount, J.L., Langley, K. and Caughey, G.H. 1999. Clustering of activating mutations in *c-kit*'s juxtamembrane coding region in canine mast cell neoplasms. J. Invest. Dermatol. 112 (2): 165-170.

Mackins, C.J., Kano, S., Seyedi, N., Schäfer, U., Reid, A.C., Machida, T., Silver, R.B. and Levi, R. 2006. Cardiac mast cell–derived renin promotes local angiotensin formation, norepinephrine release, and arrhythmias in ischemia/reperfusion. J. Clin. Invest. 116 (4): 1063-1070.

Maria T. and Zorn T. 2005. Connective tissue. In: Basic Histology, Text and Atlas. L.C., Junqueira and J., Carneiro. 11th ed. Lange Mc Graw-Hill. 176-236.

Muangsan N. 2009. DNA and RNA. In: A Handbook for Molecular Biology Researchers (in Thai). 1st ed. Chula Press. 63-82.

Meyer, D.J., Connolly, S.L. and Gan Heng, H. 2010. The acquisition and management of cytology specimens. In: Canine and Feline Cytology, A Color Atlas and Interpretation Guide. 2nd ed. R.E., Raskin and D.J., Meyer. St Louis. Saunders Elsevier. 9.

Moldering, G.J. 2010. Mast cell function in physiology and pathophysiology. Biomed. Rev. 5(1): 1-11.

Mora, F., Puigdemont, A. and Torres, R. 2006. The role of mast cells in atopy: what can we learn from canine models? A thorough review of the biology of mast cells in canine and human systems. Brit. J. Dermatol. 155: 1109-1123.

Morini, M., Bettini, G., Preziosi, R. and Mandrioli, L. 2004. C-kit gene product (CD117) immunoreactivity in canine and feline paraffin sections. J. Histo. Cyto. 52(5): 705-708.

Newman, S.J., Mrkonjich, L., Walker, K.K. and Rohrbach, B.W. 2007. Canine subcutaneous mast cell tumour: diagnosis and prognosis. J. Comp. Path. 136: 231-239.

Orfao, A., Escribano, L., Villarrubia, J., Velasco, J.L., Cerveró, C., Ciudad, J., Navarro, J.L. and San Miguel, J.F. 1996. Flow cytometric analysis of mast cells from normal and pathological human bone marrow samples. Am. J. Pathol. 149 (5): 1493-1499.

Patnaik, A.K., Ehler, W.J. and MacEwen, E.G. 1984. Canine cutaneous mast cell tumor: morphologic grading and survival time in 83 dogs. Vet. Pathol. 21 (5): 469-74.

Prihirunkij, K., Srisampan, S. and Bunnuang, U. 2007. Diagnosis of mast cell leukemia in a dog using MAPSSTM flow cytometry combined with toluidine blue (in Thai). J. Thai. Vet. Med. Assoc. 57 (3): 64-72.

Prussin, C. and Metcalfe, D.D. 2003. IgE, mast cells, basophils, and eosinophils. J. Allergy. Clin. Immunol. 486-494.

Prussin, C. and Metcalfe, D.D. 2006. IgE, mast cells, basophils, and eosinophils. J. Allergy. Clin. Immunol. 450-456.

Pryer, N.K., Lee, L.B., Zadovaskaya, R., Yu, X., Sukbuntherng, J., Cherrington, J.M. and London, C.A. 2003. Proof of Target for SU11654: Inhibition of KIT phosphorylation in canine mast cell tumors. Clin. Cancer. Res. 9: 5729–5734.

Raskin R.E. 2010. General categories of cytologic interpretation. In: Canine and Feline Cytology, A Color Atlas and Interpretation Guide. 2nd ed. R.E., Raskin and D.J., Meyer. St Louis. Saunders Elsevier. 18.

Roskoski, R. Jr. 2005. Structure and regulation of Kit protein-tyrosine kinase-The stem cell factor receptor. Biochem. Biophy. Res. Com. 338: 1307–1315.

Reggeti, F. and Bienzle, D. 2011. Flow cytometry in veterinary oncology. Vet. Pathol. 48(1): 223-235.

Rungsipipat, A., Srichat, W., Charoenvisal, N., Manachai, N., Jearanai, W., Wangnaitham, S., Tangkawattana, P. and Tangkawattana, S. 2009. Clinical evaluation of canine mast cell tumor treatment between combined vinblastine and prednisolone and single prednisolone. Comp. Clin Pathol. 18: 77–84.

Samuelson, D.A. 2007. Connective tissue. In: Samuelson Textbook of Veterinary Histology. D.A., Samuelson. 3rd ed. St Louis. Elsevier. 78-79.

Silver, R.B., Reid, A.C., Mackins, C.J., Askwith, T., Schaefer, U., Herzlinger, D. and Levi, R. 2004. Mast cells: A unique source of renin. Proc. Natl. Acad. Sci. 101 (37): 13607–13612.

Stefanov, I.S., Vodenicharov, A., Dimitrove, R. and Kostadinov, G. 2007. Density, shape and dimensions of mast cells in canine anal canal. Bulg. J. Vet. Med. 10(2): 77-82.

Thamm, D.H. and Vail, D.M. 2007. Mast cell tumors. In: Withrow & MacEwen's Small Animal Clinical Oncology, ed. S.J., Withrow and D.M., Vail, 4th ed. St Louis.: Saunders Elsevier. 402–424.

Theerawatanasirikul, S., Teewasutrakul, P, Rungsipipat, A., Wangnaithum, S., and Sailasuta, A. 2009. The prognostic value of kit expression on canine mast cell tumors by immunocytochemistry. In the Proceedings of the 2nd Federation of Asian Small Animal Veterinary Association Congress 2009 and Veterinary Medicine & Livestock Development Animal Conference 2009, Bangkok, Thailand, 3-5 Nov. 2009. P. 565.

Thompson, J.J., Yager, J.A.S., Best, J., Pearl, D.L., Coomber, B.L., Torres, R.N., Kiupel, M. and Foster, R.A. 2001. Canine subcutaneous mast cell tumors: Cellular proliferation and KIT expression as prognostic indices. Vet. Pathol. 48(1): 169-181.

Turin, L., Acocella, F., Stefanello, D., Oseliero, A., Fondrini, D., Brizzola, S. and Riva, F. 2006. Expression of *c-kit* proto-oncogene in canine mastocytoma: A kinetic study using real-time polymerase chain reaction. J. Vet. Diagn. Invest. 18: 343–349.

Webster, J.D., Kiupel, M., Kaneene, J.B., Miller, R. and Yuzbasiyan-Gurkan, V. 2004. The use of KIT and tryptase expression patterns as prognostic tools for canine cutaneous mast cell tumors. Vet. Pathol. 41: 371–377.

Webster, J.D., Yuzbasiyan-Gurkan, V., Kaneene, J.B., Miller, R., Resau, J.H. and Kiupel, M. 2006. The role of *c-kit* in tumorigenesis: Evaluation in canine cutaneous mast cell tumors. Neoplasia. 8 (2): 104-111.

Webster, J.D., Yuzbasiyan-Gurkan, V., Miller, R.A., Kaneene, J.B. and Kiupel, M. 2007. Cellular proliferation in canine cutaneous mast cell tumors: Associations with *c-kit* and its role in prognostication. Vet. Pathol. 44: 298-308.

Webster, J.D., Yuzbasiyan-Gurkan, V., Thamm, D.H., Hamilton, E. and Kiupel, M. 2008. Evaluation of prognostic markers for canine mast cell tumors treated with vinblastine and prednisone. BMC Vet. Res. 4(32): 1-8.

Weiss, D. J. 2004. Evaluation of canine bone marrow proliferative disorders by use of flow cytometric analysis of CD 45 expression and intracytoplasmic complexity. Comp. Clin. Path. 13: 51-58.

Welle, M.M., Bley, C.R., Howard, J. and Rüfenacht, S. 2008. Canine mast cell tumour: A review of the pathogenesis, clinical features, pathology and treatment. Vet. Dermatol. 19(6): 321-39.

Yancey, M.F., Merritt, D.A., Lesman, S.P., Boucher, J.F. and Michels, G.M. 2009. Pharmacokinetic properties of toceranib phosphate (Palladia™, SU11654), a novel tyrosine kinase inhibitor, in laboratory dogs and dogs with mast cell tumors. J. Vet. Pharmacol. Therap. 33: 162–171.

Yuzawa, S., Opatowsky, Y., Zhang, Z., Mandiyan, V., Lax, I. and Schlessinger, J. 2007. Structural basis for activation of the receptor tyrosine kinase KIT by stem cell factor. Cell 130: 323–334.

Zavodovskaya, R., Chien, M.B. and London, C.A. 2004. Use of Kit internal tandem duplications to establish mast cell tumor clonality in 2 dogs. J. Vet. Intern. Med. 18: 915–917.

Zemke, D., Yamini, B. and Yuzbasiyan-Gurkan, V. 2001. Characterization of an undifferentiated malignancy as a mast cell tumor using mutation analysis in the proto-oncogene *c-kit*. J. Vet. Diagn. Invest. 13: 341–345.

Zemke, D., Yamini, B. and Yuzbasiyan-Gurkan, V. 2002. Mutations in the juxtamembrane domain of *c-kit* are associated with higher grade mast cell tumors in dogs. Vet. Pathol. 39: 529–535.

APPENDICES

Appendix A

The big picture of clinical bioparameters, histopsthologic grade, CD117-IHC, CD117-ICC and PCR analysis parameters of each specimen

Specimen No.	Breed	Gender (M/F)	Age (Years)	Tumor site	Grade	IHC	ICC	FCM No.	PCR
1	M.P.	M	14.3	Abdomen	I	I	I	N/A	N
2	Golden	F	10	Trunk	I	I	I	N/A	N
3	Mixed	F	8	Abdomen	I	I	I	No.1	N
4	Pug	M	10.4	Trunk	II	II	II	N/A	N
5	Thai	M	8	Scrotum	II	III	III	N/A	N
6	Mixed	F	11	Lt. carpus	I	II	II	No.2	N
7	Mixed	F	7	Axilla	II	III	III	No.3	N
8	Golden	M	7.5	Lt. thorax	II	II	II	No.4	N
9	Mixed	M	10	Tail base	I	I	I	N/A	N
10	Golden	F	10	Back	II	I	I	N/A	N
11	Cocker	M	7	Rt.elbow	III	I	I	N/A	N
12	Mixed	F	11	Axilla	III	II	II	N/A	N
13	Mixed	M	9	Axilla	I	III	III	N/A	N
14	Mixed	M	10.7	Trunk	I	I	I	No.5	N

Specimen No.	Breed	Gender (M/F)	Age (Years)	Tumor site	Grade	IHC	ICC	FCM No.	PCR
15	S.Z.	F	12	Neck	II	II	II	N/A	N
16	Mixed	F	7.1	Trunk	I	I	I	No.6	N
17	Mixed	M	9.8	Neck	I	II	II	No.7	N
18	Labrador	M	8	Back	II	I	I	No.8	N
19	Mixed	M	12	Trunk	III	II	II	N/A	N
20	Mixed	M	8.2	Groin	III	III	I	No.9	N
21	Mixed	F	10	Axilla	III	II	II	N/A	N
22	Mixed	M	9.6	Rt. ear	I	II	II	No.10	N
23	Golden	F	10.1	Back	I	I	I	No.11	N
24	Mixed	M	10	Tail base	I	I	I	No.12	N
25	Golden	M	15	3rd digit	III	II	II	N/A	N
26	Mixed	F	12.4	Axilla	III	III	III	N/A	N
27	Terrier	F	10.1	Neck	II	II	II	No.13	N
28	Pug	M	9	groin	II	III	III	No.14	N
29	Mixed	F	10.4	Hind-limb Abdomen	II	II	II	No.15 Sorted	N
30	Poodle	M	12	Chin	II	II	II	N/A	+ve

Appendix B

DNA sequence of normal exon-11 in *c-kit* used for primer design (Downing et al., 2002)

Appendix C

Spectrophotometric measurement of genomic DNA concentration in a cell suspension

To ensure that DNA extracts existed in the solution, 5 μl of DNA solution was diluted in 495 μl sterile PCR water (Fermantas, USA; Mobio, USA). 300 μl of DNA dilution was transferred into a cuvette and measured the Optical absorption in a spectrophotometer (Shimada, Japan) at the wave length 260 λ. The sterile PCR water was used as the reference in this study. The result had shown in unit of absolute optical density (OD-ABS) which was reversely transformed into the concentration of DNA in term of μg/ml. the equation used for calculating the concentration of DNA is shown below.

$$\text{DNA Concentration} = (\text{A } 260\lambda) \times (50\mu\text{g/ml}) \times \text{Dilution factor}$$

$$\text{Dilution factor} = \frac{\text{Dilution volume}}{\text{Aliquot volume}}$$

Appendix D

Calculation of the annealing temperature, average annealing temperature and working temperature of primers

The annealing temperatures (T_m) of primers, the average annealing temperature and the working annealing temperature were established using the below equations. For this study, the annealing temperature of forward and reverse primers calculated from the equation was 66°C and 68°C, respectively. The average annealing temperature (ΔT_m) was 62°C and the final working annealing temperature (T_mW) was 57°C.

$$T_m \text{ (Primers)} = 4(G+C) + 2(A+T)$$

$$\Delta T_m = \frac{T_m \text{ (Forward)} + Tm \text{ (Reverse)}}{2}$$

$$T_mW = \Delta T_m - 5$$

Appendix E

Agarose gel preparation

Two grams of agarose gel were weighed using a laboratory-graded balance. The agarose gel was dissolved and melted in 100ml of 1X Tris-Acetate-EDTA (TAE) solution giving rise 2% W/V agarose gel solution. Further, the agarose gel solution was added with 10 μl of Ethidium Bromide (EtBr) in the ratio of 1 μl/10ml agarose gel solution (Muangsan, 2009).

Appendix F

FCM-quantitative analysis calculation

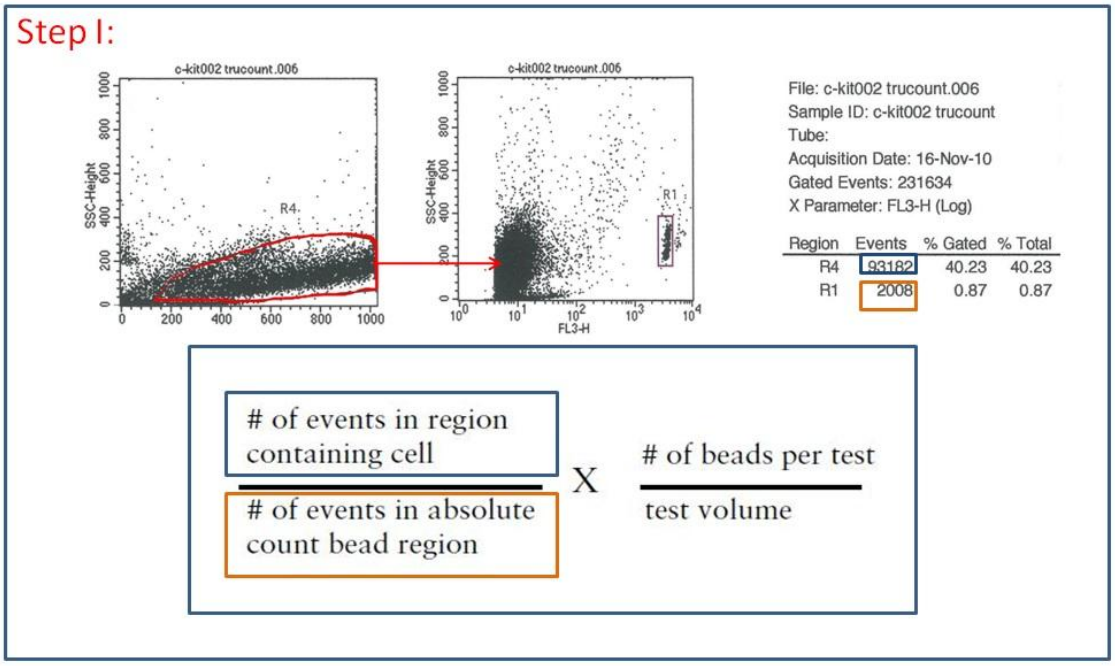

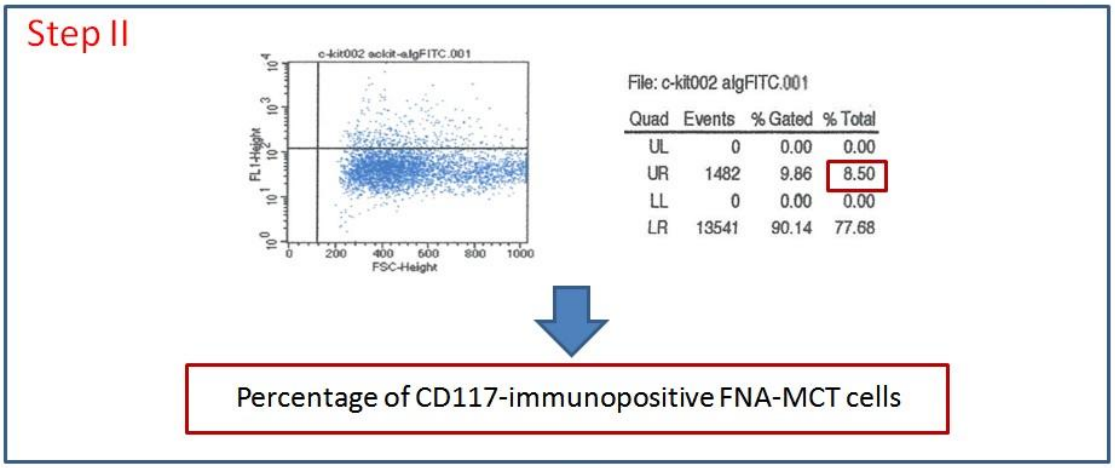

Total CD117-immunopositive FNA-MCT cells
= Result in step I x Result in step II
= cells/μl

BIOGRAPHY

Dettachai Ketpun D.V.M.

Dettachai Ketpun was born in Jan 6, 1971 in Bangkok, Thailand. He has graduated high school from Suankularb Witayalai in Bangkok, Thailand, since 1988. He has achieved his Doctor of Veterinary Medicine (D.V.M.) from Faculty of Veterinary Medicine, Kasetsart University, Thailand, since 1995. He also won a successive seat for study in Doctor of Medicine at Faculty of Medicine, Chulalongkorn University, Bangkok, Thailand in 1998 and 1999, but he did decide not to study. Since graduated, he pays his attention on small animal medicine in his private clinic and other veterinary clinics in Thailand. He has been also undertaken several opportunities to work with some international NGOs to encourage animal welfares around the world for 2 year, in 2007 and 2008. Since 2009, he has got an opportunity to study in Master of Science in Veterinary Pathobiology at Department of Pathology, Faculty of Veterinary Science, Chulalongkorn University, Bangkok, Thailand. Ultimately, He has attained his Master of Science in Veterinary Pathobiology in 2012. Recently, He plans to study in Doctor of Philosophy after accomplishing his M.Sc. in Veterinary Pathobiology. The interested field of his further study is cancer stem cells (CSC).

Presentations and publications

Development of PCR-Based for Study *c-kit* Expression from Canine Cutaneous Mast Cell Tumors FNA-Cells, 36th ICVS (International Conference on Veterinary Science) 2010, Impact conventional centre, Nontaburi, Thailand.

A comparative study on grading and *c-kit* expression of canine cutaneous mast cell tumors with standard histopathology and immunohistochemistry, 36th ICVS (International Conference on Veterinary Science) 2010, The Thai Veterinary Medical Association Under Royal Patronage, Impact conventional centre, Nontaburi, Thailand.

Pontential use of flow cytometer in fine needle aspirated-canine mast cell tumors cells on quantitative analysis and tumor grading: A preliminary study, 16th FAVA congress 2011, Federation of Asian Veterinary Associations, Cebu, Philippines.

A Tendency on the use of flow cytometric scattering pattern in canine cutaneous mast cell tumors grading, 36th WSAVA congress 2011, World Small Animal Veterinarian Association, Jeju, Korea.